ORIGINAL ARTICLE

Developments of non-conventional drilling methods—a review

Prithpal Singh [1] · A. Pramanik [1] · A. K. Basak [2] · C. Prakash [3] · Vinod Mishra [4]

Abstract
Demand for drilled micro-holes on difficult to machine materials have increased over the past years and non-traditional drilling processes are commonly used to fabricate such micro-holes on difficult to machine materials. This research investigates different non-traditional drilling processes, such as electro discharge, laser beam, abrasive water jet, electrochemical and electrochemical discharge drilling methods. Drilling mechanism, material removal rate/machining speed and surface finish have been analysed for every process. These analyses clearly show that vaporisation, melting, chemical dissolution and mechanical erosion are dominant material removal mechanism during non-traditional drilling. The understanding on electro discharge, laser beam and abrasive water jet drilling are more developed than that of electrochemical, electrochemical discharge and hybrid drilling processes.

Keywords Micro-drilling · Non-conventional drilling · Electro discharge drilling · Electrochemical drilling · Ultrasonic drilling · Water jet drilling · Laser drilling

1 Introduction

Drilling is a basic processing step in manufacturing industries to fabricate different parts as well as for numerous structural applications [1, 2]. With the advance of manufacturing technologies, demand for holes smaller than 0.1 mm has been high in automobile and aerospace industries on applications such as turbine blades, injection nozzles, etc. On the other hand, medical appliances require accurate micro-holes [2]. Drilling micro-holes on materials with high hardness and brittleness can be a challenge for most conventional drilling methods or impossible in some occasions [1]. The key problems with conventional drilling methods include tool wear, burr formations and lower material

removal rates. In addition to that, hard to machine materials incur high cost by conventional means due to frequent replacement of tools and high cost of skilled labour. Therefore, in order to increase the capability to drill holes in complicated shapes and hard to machine materials, non-conventional drilling processes were introduced [3]. Manufacturing companies have adapted non-conventional drilling methods for their attractive features like absent of burrs, high material removal rate, high precision holes, ability to drill into hard materials such as, titanium alloys, metal matrix composites (MMC), absence of mechanical stresses from conventional tools and ability to produce non-circular holes [4]. Drilling of holes in materials using non-conventional methods involve removal of materials not by the action of applied force but by the action of thermal, chemical, electrical and abrasive effects; or even combined effects (hybrid) of these methods [2].

Many researches focusing on non-traditional drilling processes are available in the literature. However, the available information is not properly linked, and a complete picture of the processes is not available, though these are imperatively required to advance the knowledge and proper selection of suitable drilling method. To address these issues, this paper investigates the appropriateness of different non-traditional drilling processes. Every non-traditional drilling process below has been analysed based on (a) material removal mechanism, (b) cutting speed/material removal rate and (c) surface finish and dimensional accuracy and other parameters which

✉ A. Pramanik
akprama@yahoo.com; alokesh.pramanik@curtin.edu.au

[1] School of Civil and Mechanical Engineering, Curtin University, Bentley, WA, Australia

[2] Adelaide Microscopy, University of Adelaide, Adelaide, SA, Australia

[3] School of Mechanical Engineering, Lovely Professional University, Phagwara, India

[4] CSIR – Central Scientific Instruments Organisation, Chandigarh, India

are important for a given method. All parameters considered in this study are important scientifically, economically and assessing the latest developments, performance and efficiency of the considered non-traditional machining methods. Material removal mechanism describes the up to date understanding of the specified methods and reveals if there are any underlying issues related to that methods. Cutting speed/ material removal rate is very much related to how quickly a method can perform a given task. Cutting speed tells us about the efficiency of the method as well as its suitability for a given application. Surface finish and dimensional accuracy is a measure of performance of any method. If any method gives inferior surface and dimensional accuracy compare to other methods at similar machining conditions, then the performance of the first method is worse than that of other methods. Thus, the method needs to be fixed and more researches are required to improve it. Having said that, this paper provides the contribution of many research works, advancement of process understanding, current state of the art knowledge and trends in research to advance the technologies through the discussions on several output parameters of different methods. The aim of the present work is to link all the understanding achieved by different researchers and analyses those facts scientifically and systematically to provide a global scenario on machining of materials by non-traditional processes.

2 Different types of non-conventional drilling methods

There are number of non-conventional drilling methods available to drill holes in different materials ranging from common metallic alloys to hard-to-cut materials. The reason behind the evolution of number of non-conventional method is that, each of the developed method has its own pros and cons and thus, no single method can satisfy all the required objectives of the given situation. The most common non-conventional drilling methods are as follows:

(i) Abrasive water jet drilling (AWJD): This method includes abrasives mixed in water jet where materials are removed by high pressure through a slurry medium. Abrasive water jet drilling on the other hand is a process with the absence of heat and abrasive particles are combined with water at high speed and pressure to erode material from workpiece [5]. Ultrasonic drilling is a non-traditional drilling process used these days for conductive and non-conductive workpiece material and able to drilling workpiece with a hardness higher than 40 HRC [6].

(ii) Thermal drilling: In this technique, a heat source is used to remove material by melting and vaporising. Example

of this is laser drilling (LD) that uses a focused laser to generate heat at a given point [7]. Heat source can also be applied from on electrical sparks-such as electrical discharge drilling (EDD) involve material removal through the generation of a sparks between the tool and workpiece gap in the presence of dielectric fluid [2]. Micro-EDD is commonly used in industries that desire holes with high precision and tolerances mainly for materials such as titanium [8].

(iii) Chemical form of drilling: Examples of such techniques are electrochemical drilling (ECD) that involve anodic dissolution where a tool (cathode) and workpiece (anode) forms an electrolytic cell with appropriate electrolyte circulating through the middle of the anode and cathode. Based on Faraday's law, small holes are created by dissolving the anode when adequate amount of voltage is fed between the minute spaces of the tool and workpiece in the electrolyte. Electrochemical process uses a weak acidic solution known as an electrolyte to produce small holes that utilizes a fixed amount of anodic dissolution [9]. Shaped tube electrolytic drilling (STED) is a modified version of ECD, where holes are created by using controlled depleting that can only be conducted on a workpiece that is an electrical conductor. The depleting action occurs in an electrolytic cell that is created by a cathode (i.e. a metal electrode charged negatively) and an anode (i.e. the workpiece) that is charged positively. The anode and cathode are divided by an electrolyte which is an electrically conductive fluid [9]. Capillary drilling consists of a drill tube which is actually a glass capillary, where electrolyte flows through with a pressure of 3–20 bar [9]. Material is removed by the inner diameter of capillary that acts as an electrode. As for electro stream drilling, material is removed by electrolytic dissolution as the flow of electrolyte impinges the workpiece [9]. Lastly, in jet electrolytic drilling, the hole is created by a jet electrolyte with a pressure of 10–60 bar that strikes the workpiece [9].

(iv) Ultrasonic drilling (USD): This method utilizes the energy of ultrasound that is used to vibrate cutting medium to drill relatively shallow holes in low ductile materials. It is a form of mechanical drilling that fabricated holes without any recast layer and alteration of microstructure of workpiece materials.

Different aspects of above-mentioned drilling techniques are explained in details in subsequent sections.

3 Abrasive water jet drilling

Abrasive water jet is a non-conventional drilling method process that erodes material out of the workpiece through a

stream of water at high velocity that consists of abrasive particles which are added through the outlet tip of the nozzle [10]. The addition of abrasive particles increases the range of materials that can be drilled such as materials with high hardness [11]. The different types of abrasive particles are aluminium oxide, silicon carbide, sodium bicarbonate, dolomite or glass beads with different sizes are used [12]. The typical abrasive particles used for drilling is garnet of size mesh 80 to 220 [11, 13], which are around 66–177 μm [14] with a mass flow rate of around 1.36 kg/min [11, 13]. As shown in Fig. 1, water at a high pressure and velocity enters the mixing chamber while the abrasive particles simultaneously enter the mixing chamber. Air, water and abrasive particles form a mixture that exits the nozzle with high kinetic energy that erode the workpiece [10, 12, 15]. Abrasive water jet drilling (AWJD) is capable to obtain good quality holes without any thermal damage when compared to other non-conventional drilling process that involve the application of heat (EDM or LBM). For holes having diameter larger than the jet, the jet moves in a circular path to machine the hole [16]. Holes at different angles can also be drilled using AWJ [11, 16]. This process allows the drilling of non-conductive and reflective materials as well [17].

3.1 Mechanisms

As mentioned above, the mixture containing abrasive particles and water acts as cutting tools that aids the erosion of the workpiece. Three different steps in AWJD are (a) piercing, (b) trepanning and (c) drilling steps [18, 19]. During piercing step, waterjet containing abrasives moves at a high velocity to pierce into the workpiece. Following that, the return flow interrupts the input jet flow which travels radially outward at high pressure and erodes the materials on the inner side wall of the hole through abrasion. Figure 2 below illustrates the piercing process by AWJD. After piercing process, waterjet cuts through the material following a circular path based on the diameter required by the manufacturer [13, 18]. The second step increases the size of the holes that were produced in piercing and this process is known as the trepanning step. The drilling step produces blind holes where the interior shape of the holes as well as depth is not easily controlled [19].

In addition to the slurry mixture, high-pressure air is likewise added into the tank which excites the jet flow to allow high-pressure abrasive particles to erode the workpiece at a high impact force. Ductile erosion and brittle erosion are the two different types of erosion process. Ductile erosion is where the abrasive particles gradually remove the workpiece material which will then lead to volumetric material removal. Brittle erosion is also known as a cracking process, whereby the fragments of the workpiece are removed by the joining point of the lines of cracks surrounding the abrasive particles [20]. A ring-shaped backflow area covering the flow by the jet is turbulent, (disordered jet with high pressure), will then aid the removal process by abrasion. The jet fluid consists of both water, air and abrasive particles as well as the fragments of the workpiece [19]. It can be observed that a cavity is formed by the abrasive particles that erodes the workpiece at the desired pressure. Following the formation of the cavity, the jet will be able to extend to a definite depth. The abrasive particles are accelerated by the waterjet to a high speed so that the thrust force and change in motion of the abrasive particle can erode the workpiece [12]. Figure 3 shows the different parameters that affect the material removal rate and generation of surface roughness of drilling process of AWJD process.
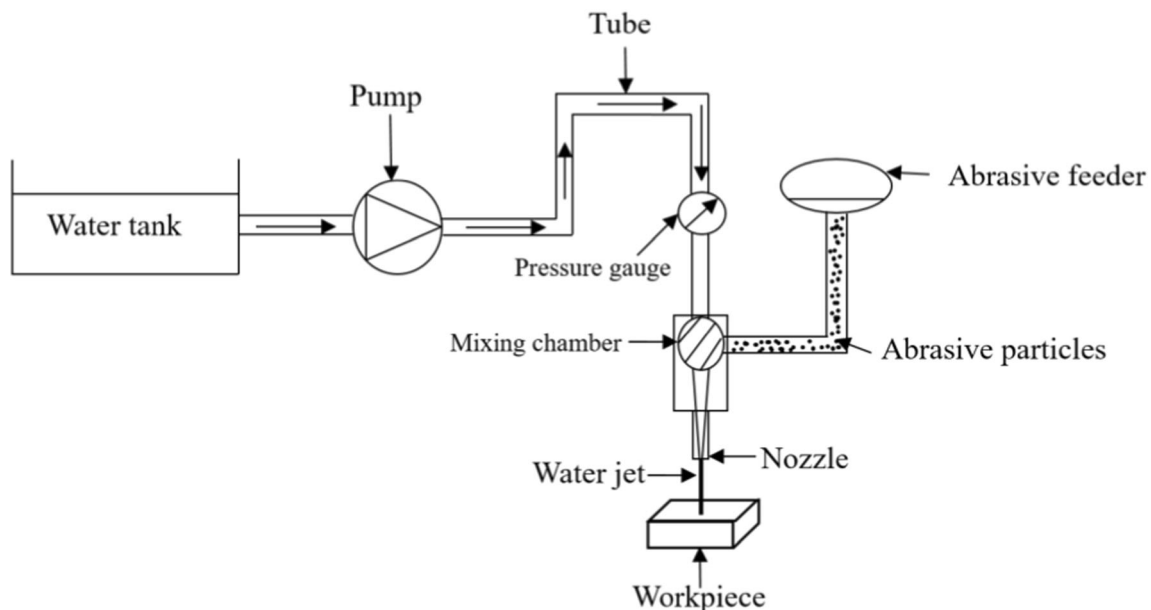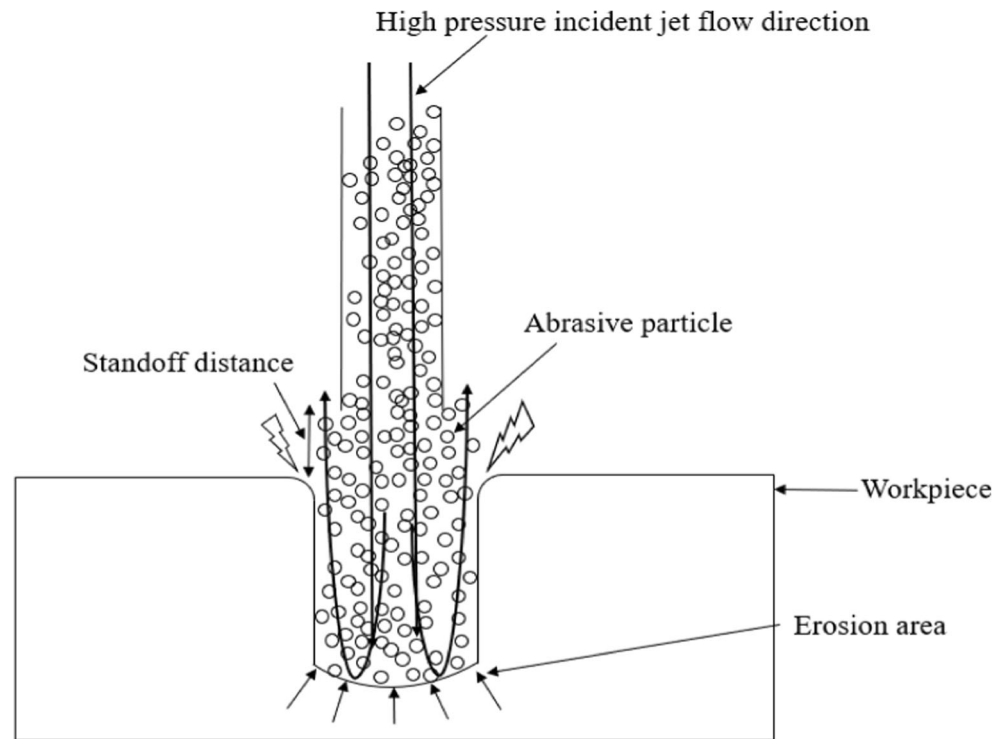

**Fig. 1** Schematic diagram of abrasive water jet drilling process [10]

Fig. 2 Illustration of abrasive water jet drilling mechanism

3.2 Material removal rates

The drill speed during AWJD is influenced by key parameters such as workpiece type, pressure level of the water and the mass flow rate of the abrasives as shown in Fig. 3. To decrease the time taken for drilling, increase of pressure and abrasives flow rate are required [11, 13, 16]. Though Hashish and Whalen [11] did not reported any trend between drilling rate and abrasive flow rates, however, it can be seen that the drilling speed is directly proportional to abrasive flow rate. Other parameters such as standoff distance affects the drilling rate; the larger the standoff distance, the slower is the drilling rate [21]. A study conducted by Akkurt [16] report that drill time taken for different materials with different thickness where the processing parameters were unchanged as shown in Fig. 4. It shows that different materials have different drilling time and that pure aluminium is able to be drilled at the fastest compared to AISI 304 stainless steel. As the thickness increases from 5 to 10 mm, drilling time increases by 255% and 300% for aluminium and steel, respectively. Reason for the increase in drilling time is because of the pressure loss, decrease in the abrasive performance and build-up of chips and abrasives in the cutting zone. Hunt, Burnham and Kim [22] noted the effect of pressure, flow rate and type of abrasive used to control the duration taken to pierce the workpiece. It was evident that piercing time decreases with higher abrasive mass flow
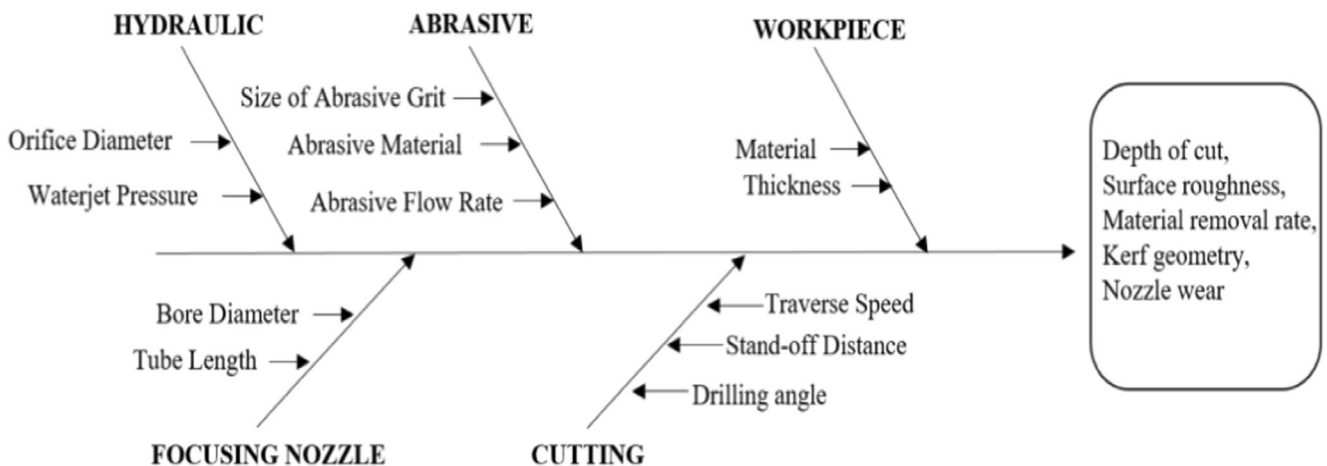
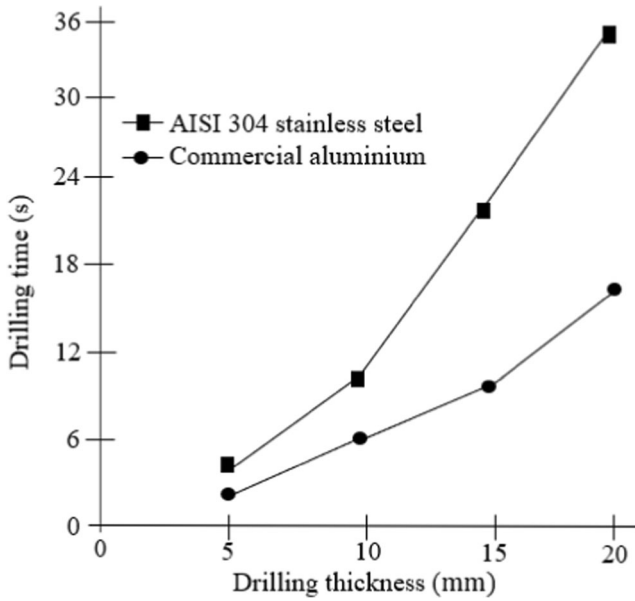**Fig. 3** Parameters influencing abrasive water jet drilling [10]

Fig. 4 Drilling time of aluminium and AISI 304 stainless steel with various thickness [16]

rate and higher pressure because of the higher mass momentum that increases the impact force responsible for the erosion of the workpiece as presented in Fig. 5. Hashish [11] found that the denser abrasives such as WC had slower drill rate compared to olivine and garnet due to the lack of high acceleration needed to reach high speeds. Olivine was found to have a faster drill rate compared to garnet and also the coarser olivine was found to have higher drill rates than finer olivine, as larger the abrasive particle, larger is the surface area of the particles, hence increasing the area of erosion.

3.3 Hole characteristics and surface finish

Key parameters such as type of workpiece, pump pressure, traverse speed and standoff distance affects hole taper [23, 24]. A study conducted by Hamatani et al. [23] showed that stand-off distance is a function of hole taper ratio for both silicon carbide and titanium diboride where the stand-off distance is directly proportional to hole taper ratio. The possible reason is that the larger the distance, the larger is the area of jet flow on workpiece, hence increasing hole taper ratio. Another study [25] conducted on drilling with abrasive waterjet in titanium shows that taper angle increases with traverse speed as shown in Fig. 6. At lower traverse speed, optimal machining of jet varies, which is possibly due to low traverse speed of the waterjet, as fewer abrasives would impinge onto the workpiece surface to cause erosion; hence, the initial interior taper hole surface reduces [25]. The quality and shape of holes drilled by abrasive water jet relies on the duration needed for drilling and the shape of the jet where drilling rate refers to the duration of piercing and the jet structure refers to the hydraulic, mixing and abrasive factors while also taking to consideration the return flow that also affects the hole shape [11]. Liu [13] stated that special profile holes can be drilled by AWJD as shown in Fig. 7 where elliptical holes drilled in Nickel aluminide vane.

Liu and Schubert [26] drilled holes in phenolic composite by using abrasive water jet as shown in Fig. 8, where surface cracks are observed. The experiment was conducted using 0.25 mm nozzle diameter at 276 MPa pump pressure with 120 mesh garnet. Note that tensile strength of phenolic composite is relatively low which is about 60 MPa. A study conducted by Liu [13] showed that materials with low tensile strength are prone to cracking.
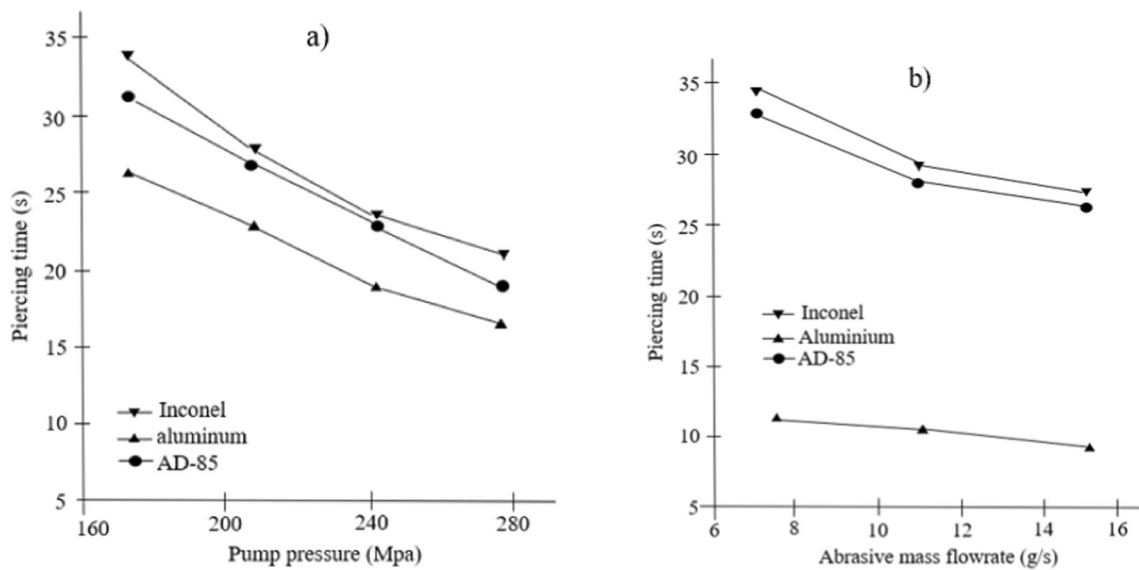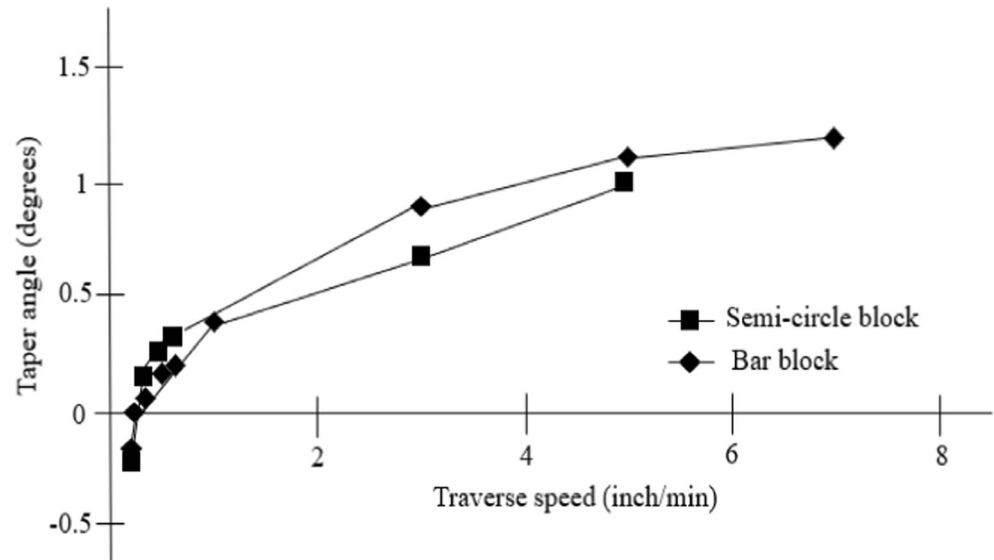

Fig. 5 Influence of (a) pump pressure with constant abrasive flow rate at 11.3 g/s and (b) abrasive mass flow rate on the drilling time of various materials [22]

**Fig. 6** Effect of transverse speed on taper angle [25]

Phapale et al. [27] conducted AWJ drilling in CFRP where both holes were drilled with abrasive garnet with a mass flow rate at 5.4 g/s and standoff distance of 1 mm at water pressures of 1000 and 2000 bar for holes presented in Fig. 9a, b respectively. Delamination extent can be calculated by subtracting the drilled exit hole size from the maximum diameter of the damaged region. The hole shown in Fig. 9a did not suffer any cracks of delamination however the hole in Fig. 9b suffered delamination extent of 2.30 mm. The suspected reason for the increase in delamination extent is because of the water pressure which contributes to a higher thrust force striking onto the workpiece and causes a slight deformation at the exit of the hole. The standoff distance was found to be directly proportional to the delamination extend. But only a minor increase of the delamination extent is discovered with the rise of abrasive flow rate in this study [27].

The common issues encountered during the drilling of holes by AWJ are shadow hole, teardrop, crack, chip, gouging, pit and delamination [11]. The shadow hole is caused by an overstated type of tear drop where two holes show up on a surface. Both teardrop and gouging occur due to the rebound effect of the jet. Pitting happens on the interior surface of the wall due to the large abrasive impact. Delamination happens most commonly on ceramic-bond-metal interface [11].

Hashish [28] reported that damage occurs due to quick and sudden loading of water, and hydrodynamic pressure. This

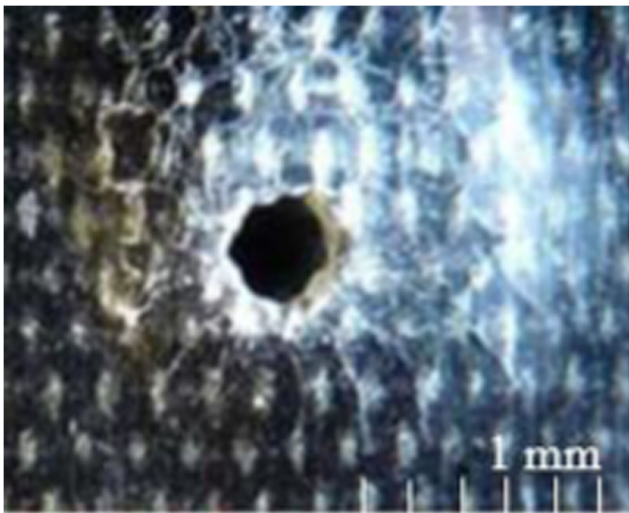**Fig. 7** Elliptical holes drilled by waterjet on Ni/Al vane [13]
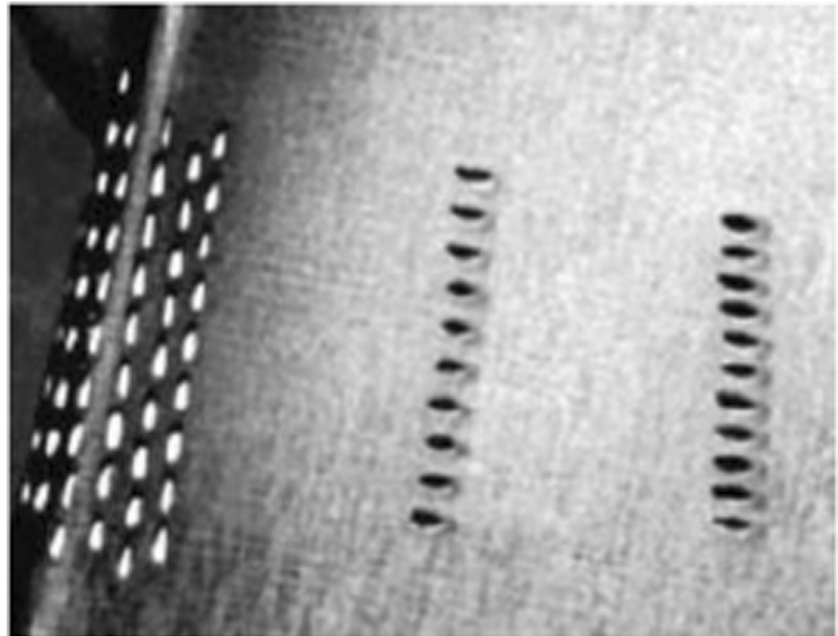
Fig. 8 Top of hole pierced on phenolic composite [26]

Fig. 10 Surface roughness of drilled hole: **a** no back up plate and **b** with back up plate [27]

can be prevented by decreasing the pressure or the diameter of the jet. Materials that have low tensile strength are prone to cracks and delamination [13, 26]. Delamination appears to be a huge problem in abrasive water drilling in composites. Phapale et al. [27] suggested few methods to reduce delamination such as by using backup plates, pre-drilled holes and conduct drilling after submerging workpiece fully under water. Results show that the best method to regulate delamination is the backup plate as it is the most successful way as the deflection at the bottom hole decreases and, hence decreasing delamination.

Phapale et al. [27] reported that the roughness of drilled hole in CFRP is directly proportional to water pressure, stand-off distance and abrasive flow rate. The surface roughness of the drilled hole is shown in Fig. 10 with a backup plate and without backup plate, where at 2000 bar, the flow rate of the abrasive slurry was at 8.87 g/s with a standoff distance of 2 mm and at 2500 bar, the abrasive flow rate was at 9.7 g/s with a standoff distance of 3 mm. The surface roughness appeared to be lower for the hole with backup plate. Zhang et al.
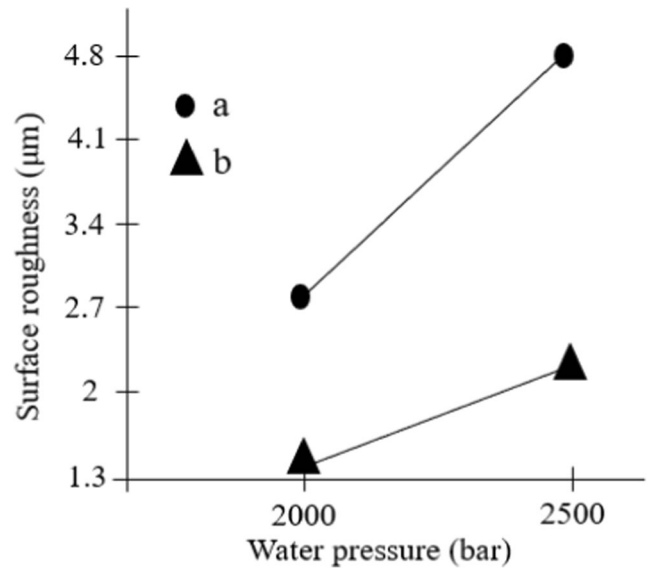
[25] also achieved similar outcomes. Surface roughness is heavily dependent on drill speed, which is possibly because, when the speed is low, surface quality is better as abrasive particle would not cause high abrasion on the surface which will then reduce surface roughness [25, 29]. Abrasive waterjet drilling does not change the microstructure of the materials [16]. Figure 11 shows an example of microstructure image taken of 1030 low-carbon steel after AWJD.
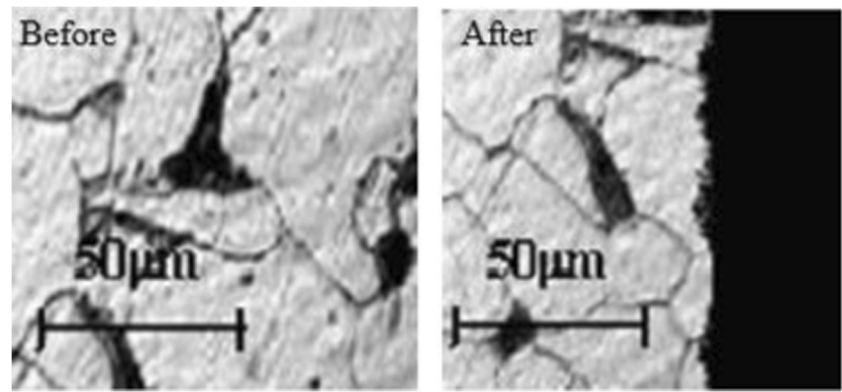
4 Laser drilling

Laser drilling process removes materials by thermal energy. It is a contactless drilling process with no tool wear and not restricted to only conductive materials. Laser drilling uses a thermal heating source to melt and vaporize the workpiece [30]. Laser drilling is a great choice for creating holes with minimum hole taper and great roundness as these two

Fig. 9 Back hole of carbon fibre reinforced plastic (CFRP) with different pressures: **a** 1000 bar and **b** 2000 bar [27]
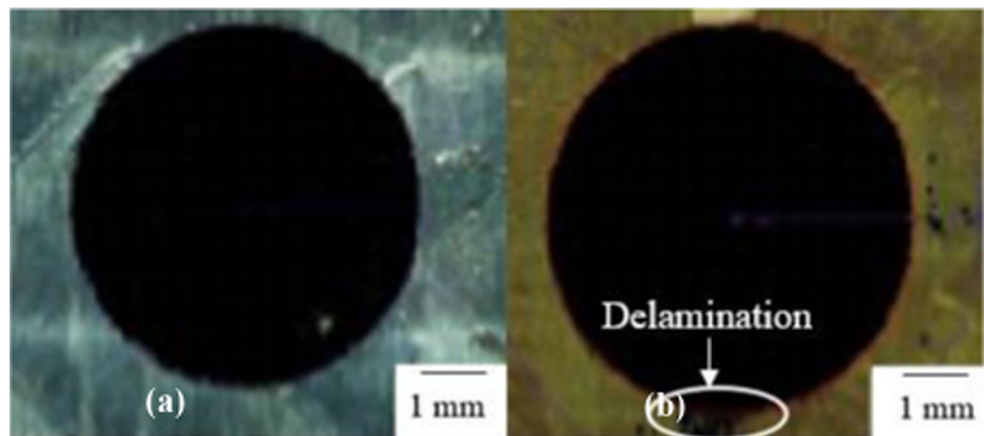
Fig. 11 Microstructure captured at the side of the hole surface of S1030 low-carbon steel [16] with comparison of initial state

characteristics are always desired when drilling holes [31]. Figure 12 shows the schematic of a typical set-up of a laser drilling process. The advantages of using laser drilling are contactless drilling, high precision holes can be drilled, repeatability, high flexibility, no chip or burr problems, high production rates, large aspect ratio of holes achievable, able to drill a range of materials from hard to soft and hole diameters range from 0.2 μm to 1.5 mm holes by percussion drilling [33, 34]. Laser drilling process is normally for drilling tiny holes at fast drilling rates and used in aerospace industries for aerospace component such as turbine blades, guide vanes and casings [30, 31, 33]. However, laser beam heating on materials are generally influenced by the thermal properties of the workpiece rather than the material mechanical characteristics and laser beam energy density [35]. Hence, materials with low conductor of heat are much preferred. Brittleness and hardness of material do not really have much effect on laser drilling

[36]. Heat energy from laser strikes onto the surface of workpiece through irradiation [34]. CO_2 and Nd:YAG are two typically used lasers in the industry; however, Nd:YAG has been reported to drill faster compared to CO_2 laser system [34, 37].

4.1 Drilling mechanism

Material removal mechanism during laser drilling can be divided in following stages: (i) melting/vaporization of material and break down of chemical bonds, (ii) cooling down of material [36]. The difference between laser beam and normal light is the existence of photon energy in laser beam [36, 38]. When laser radiation strikes on workpiece, electrons that are present in laser are triggered by the photons which then produces heat and absorbed by the material that follows Lambert's law, causing ablation of the material [39]. The Beer-Lambert law explains the absorption of light on material and influenced by distance

Fig. 12 Nd:YAG laser drilling schematic diagram [32]
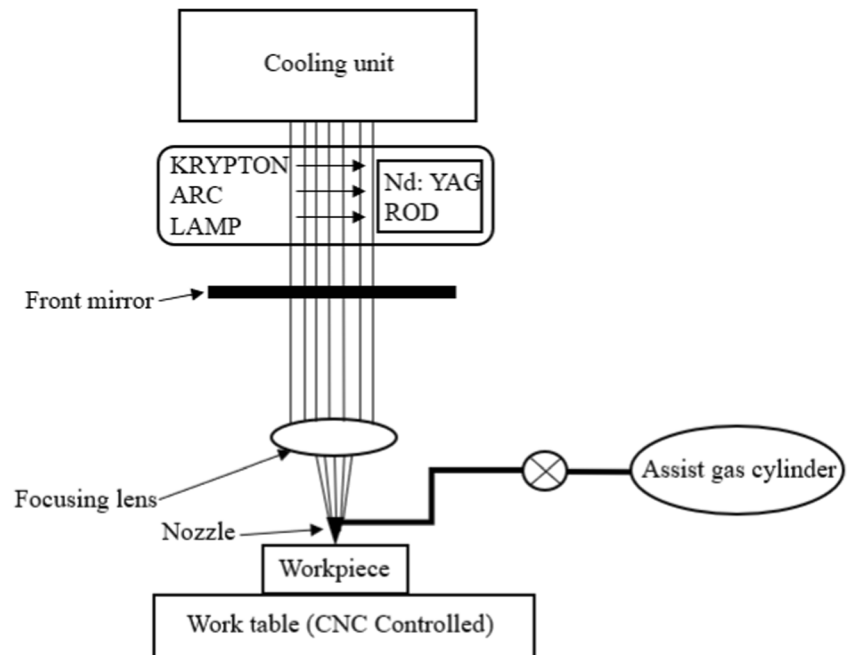
of which the workpiece is moved when laser beam concentration [39] (R.E. Wagner). Figure 12 represents the schematic diagram of laser drilling system where the incident laser beam is transmitted through focusing lens onto target material in the form of thermal energy to heat up the surface. As a result, the target material melts and vaporizes, which are influenced by target material and concentration of laser beam. Cooling unit is used to cool the machine to prevent overheating of the lamp and Nd:YAG rod. Melted metal is then cleared away by assist gas [34]. However, different types of material have different absorption of heat energy from laser beam. For example, opaque materials absorb the energy at top layer of workpiece and the heat travels to other zones of the work piece through conduction. Vaporisation of material is heavily influenced by material conductivity and mass to volume ratio of laser-beam energy. In order for the material to be vaporized, material first will absorb heat from laser till the temperature of the material rises to its melting point. Subsequently, heat will be absorbed at a steady rate till it reaches the entire material and finally heated up again at a steady rate till vaporization temperature is achieved [35].

Ready [40] proposed that in order to achieve continuous vaporization of workpiece, energy of the laser beam has to be at a steady-state condition with high energy density, acting on the top layer of workpiece. The surface will then recede at fixed velocity. Whereas for translucent materials, only partial heat energy from laser will be consumed by the surface, while rest of the layers will be heated through absorption. This depends on how well the surface can absorb heat energy that is the materials' thermal absorption coefficient. Dabby and Paek [41] found that ablation occurs on top surface of the workpiece. The layers of the workpiece below top surface will increase in temperature through absorption over vaporization temperature, which will allow the expulsion of materials during laser drilling process.

The different techniques used in laser beam drilling can be separated into static and dynamic drilling. Single pulse drilling and percussion drilling can be classified under static drilling while trepanning and helical drilling are classified under dynamic drilling [34, 38]. In static drilling, substrate and laser beam is at a fixed position and the expulsion of workpiece is caused by number of pulses. The difference between single pulse drilling and percussion drilling is the number of successive pulses in contact with workpiece, where only one pulse is used for single pulse drilling and multiple pulses are used for percussion drilling. Figure 13 illustrates drilling mechanism using percussion drilling. Dynamic drilling focuses on laser motion from the middle of the hole to circumference. Dynamic drilling consists of trepanning and helical drilling, where erosion of the substrate occurs by vaporisation and material is removed from helical drilling is similar to trepanning except that helical drilling consists of optical wedges for the inclination of laser beam of up to 5° [34, 38].

4.2 Material removal rate

Material removal rate (MRR) of laser drilling is mainly dependent on the energy of laser beam, and thickness and workpiece type. The various parameters shown in Fig. 14 affects surface roughness and material removal rate during drilling process. The thermal diffusivity and absorption coefficient of the materials are the main effects on drill speed. On the other hand, how fast or effective the heat can transfer in the substrate is important for ablation process [42]. For example, a study conducted in [43] using pulsed Nd:YAG laser shows that with increased pulse energy, drill speed increases. This is fair because laser with higher energy will result in higher pressure striking on the workpiece surface and hence increase material removal rate. Figure 15 shows linear effect of pulse energy on mean drilling speed and it is evident that titanium can be drilled fastest as compared with nickel, EN58B (steel) and tantalum. This is because titanium has lower thermal diffusivity and higher absorption coefficient, and hence temperature gained will be higher as compared with the other materials [43]. Yilbas [44] also did another experiment and obtained similar results that with increased energy, drilling rate increases. Figure 15 shows the effect of pulse length on mean drilling speed. As pulse length increases, drill speed decreases. This is because with low pulse, at pulse off time, there will be no laser emitted, hence temperature of the workpiece will cool down and hence will not be as effective as a high pulse frequency where temperature of the work piece will keep increasing leading to higher material removal rate of titanium, nickel, tantalum and EN58B. Similar results were obtained by Ghoreishi et al. [31] using Nd:YAG laser. Tam et al. [30] also found that with increased pulse energy, drilling time reduces and with longer pulse duration, drilling time of Inconel 718 increases.

Yilbas [43] concluded that with greater thickness of material, material removal rate increases due to the increase in pressure impinging on crater; however, different materials act differently on how the thickness affect drill speed based on their properties. Similar results were obtained by Mishra and Yadava [45] where drilling speed increased with the rise of material thickness. Tam et al. [30] noted that pulse shape affects the drilling speed. Double and triple pulse is preferred compared to single pulses due to better performance. This is because the spiked pulse gives out higher peak powers than continuous pulse, hence materials removed by double and triple pulse are higher [30]. However, focal position did not affect drilling time. Another study conducted by Roos et al. [46] obtained similar results and achieved better quality holes when drilling using normal pulse and pulse train. Better results were obtained using pulse train, it is because during short intervals of normal pulse, material cools down and solidifies and hence molten material chokes the hole. However, for pulse train, every spike interval is at 0.5 μs, whereas for

Fig. 13 Material removal
illustration during laser drilling
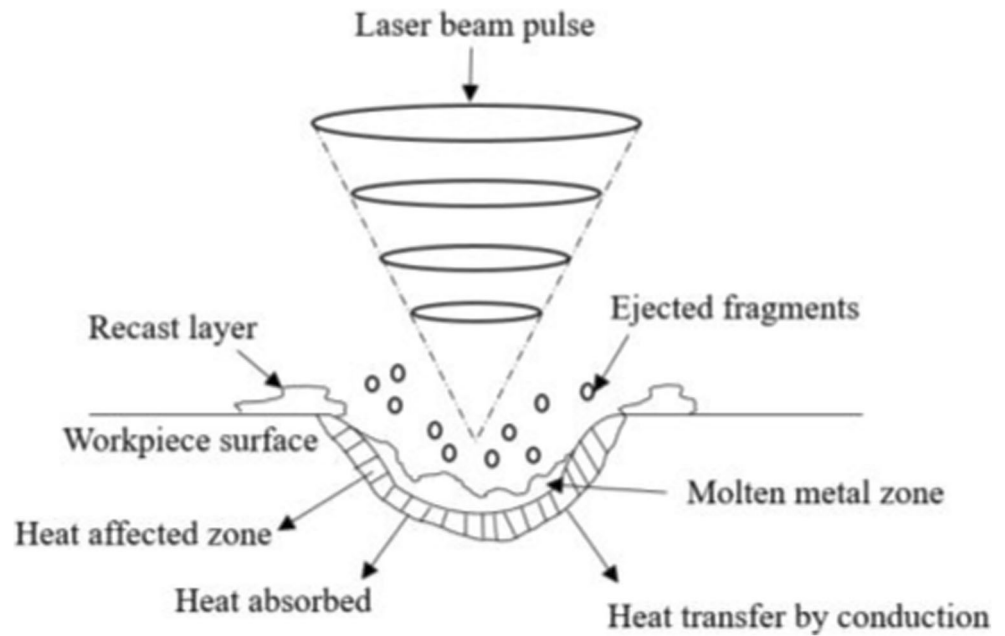
normal pulse it is at 200 μs. Hence during pulse train, vapour in the hole will leave before the next pulse. The effect of pulse energy and pulse length on mean drilling speed is presented in Fig. 17.

4.3 Hole characteristics and surface finish

The hole quality drilled by laser drilling depends on the parameters listed in Fig. 14. The quality of the holes can be characterized as hole taper, inlet and exit cone, barrelling, surface roughness and extent of heat affected zones [34]. The main parameters such as workpiece material and its thickness, pulse energy and pulse frequency seem to have significant effect on the holes based on the studies conducted. The holes drilled are normally not impeccably conical shaped as the taper depends on hole depth [47]. An example of an ordinary hole is shown in Fig. 16. Barrelling is caused by the

existence of confined hot plasma from vaporized material. Taper is present because of the erosion caused by vaporization of material. Recast is the original material that was not fully vaporized, usually located around the hole or the interior surface of hole [33].

According to Wagner [35], depth of hole is approximately proportional to laser-beam energy density, as with higher energy density, faster the vaporization temperature of the material is reached hence material removal will increase. A similar trend between energy of the pulse and hole depth was observed [34]. Both studies conducted by Gautam et al. [34] and Yilbas et al. [42] discovered that hole taper increases when the energy increases. Wang et al. [48] performed laser drilling on structural ceramics using Nd:YAG laser and found the effect of pulse energy on the circularity of hole. Figure 17 depicts the relationship between pulse energy and rate of which material is removed.
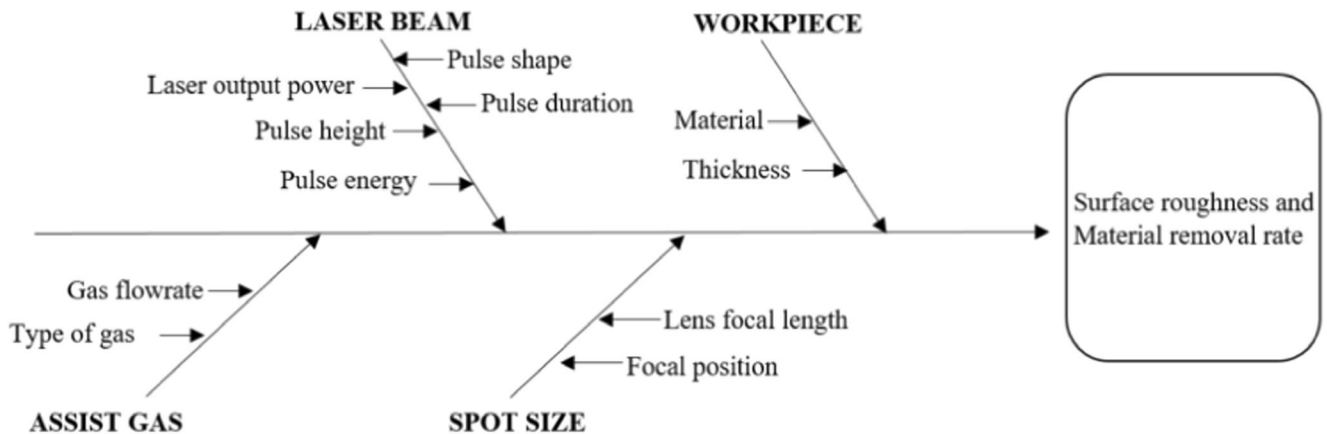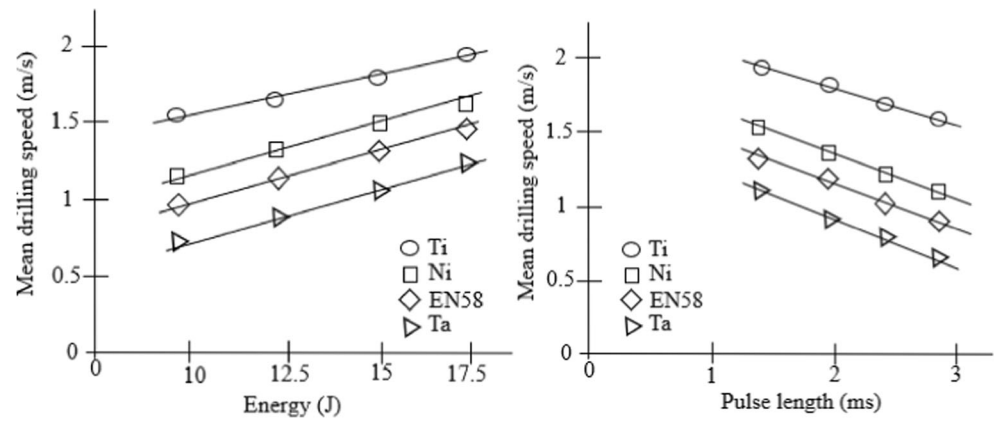

Fig. 14 Parameters affecting surface roughness and material removal rate during laser drilling [30]

Fig. 15 Effect of pulse energy and pulse length on mean drilling speed [43]


Wang et al. [48] discovered that laser power is directly proportional to taper angle. As laser power surges, hole taper angle decreases. Ghoreishi et al. [31] obtained similar results where hole taper can be reduced with higher peak power. This is because laser beam penetrates through material and enlarges exit hole resulting in exit hole being larger than entrance hole. Ghoreishi et al. [31] also discovered that with higher pulse frequency, hole taper can also be reduced due to consistent pressure striking on workpiece surface enlarging exit hole. However, with lower frequency, circularity of hole can be improved; this is because during pulse off time, material has a longer time to cool down and solidify which avoids irritation and any irregular movement of fragments during drilling. The hole taper differs for different materials due to their thermal properties, as some material transfer's heat through their layers faster than other materials [31]. Similar results were found in Bandyopadhyay et al. [47], where the taper angle reduces with growing pulse frequency.

Yilbas et al. [42] found that with increased focus setting, geometry of hole can be enhanced; however, ideal focus on workpiece is different for different materials due to different thermal properties. Another similar study was conducted by Ghoreishi et al. [31] where the focal position affects the size of holes, where larger holes can be achieved when nozzle is nearer to substrate with higher intensity, as mechanical load applied on work piece is higher with higher laser intensity.

Extend of heat affected zone (HAZ) allows to determine the extent of damage caused by heat on workpiece produced by high energy beam [49]. Studies conducted by Mishra et al. [45, 49] showed that the extent of heat-affected zone is proportional to

Fig. 16 Typical characteristics of hole drilled using laser beam [34]
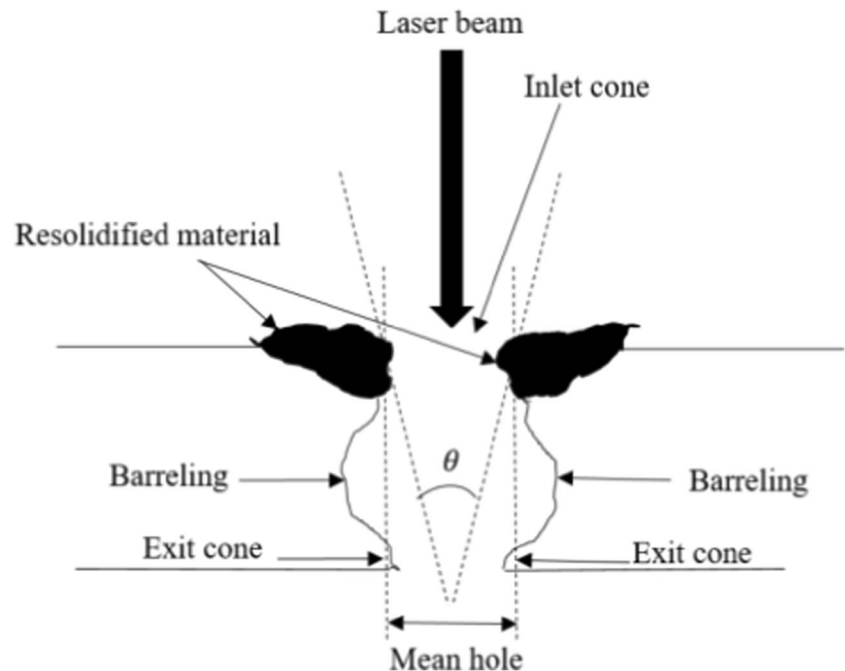
Fig. 17 Effect of energy concentration on circularity of holes (Wang et al. 2017)
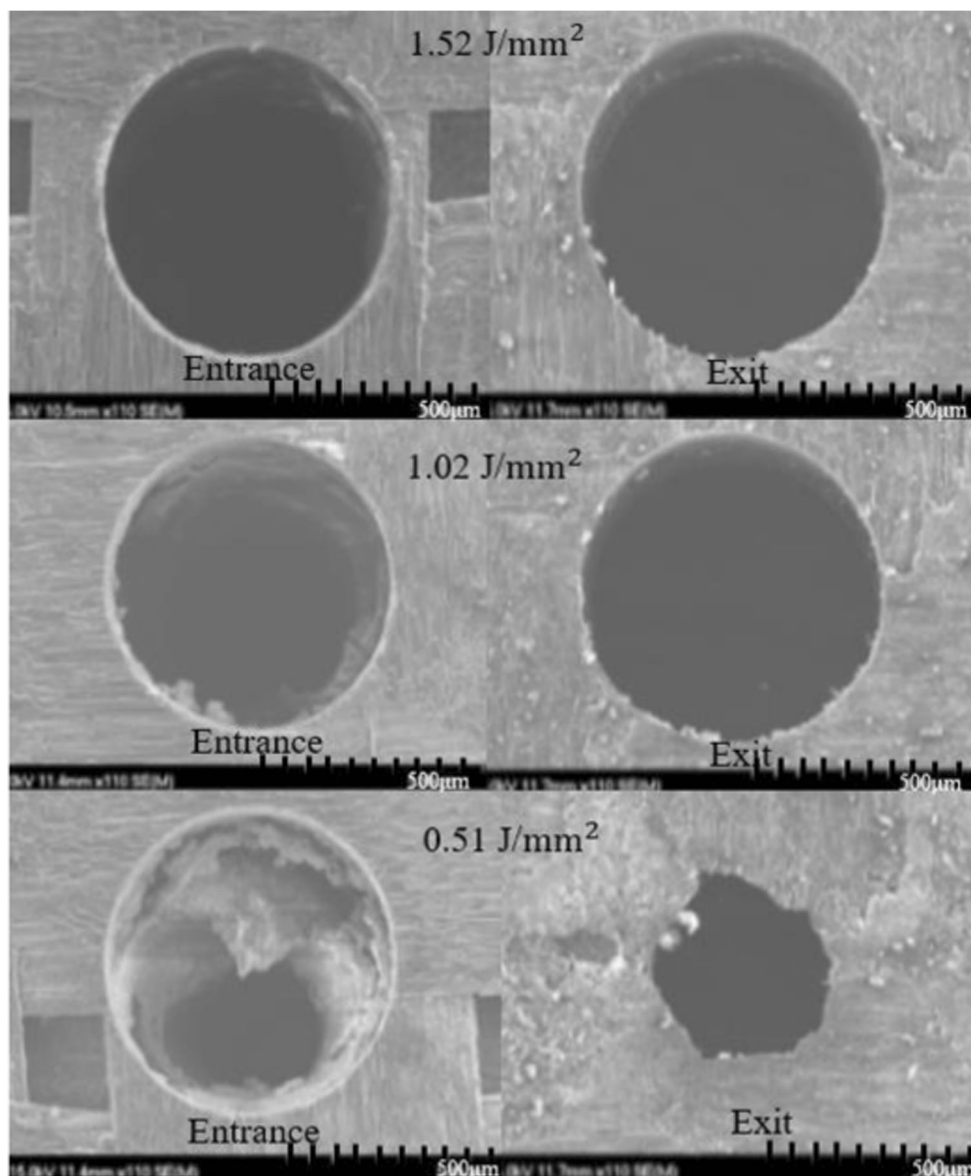

pulse width and frequency but inversely proportional to peak power. As pulse frequency increases, heat-affected zone increases because the interval between the pulses are short, hence large diffusion will form a large HAZ region. However, extent of heat-affected zone decreases when peak power increases is because when peak power is high, thermal energy striking on workpiece is high and heat will be accumulated on substrate surface. According to the study conducted by Wang et al. [48], it is possible to reduce heat-affected zones by increasing pulse frequency. Another method to reduce heat-affected zones is [50] underwater drilling revealed absence of debris, heat-affected zones and cracking.

With high pulse energy, drill speed and circularity of holes are found to be excellent. However, a study by Vora et al. [51] discovered that surface roughness is directly proportional to

laser beam energy. Kamlage et al. [52] experimented deep drilling holes of metals on stainless-steel plate using sapphire laser system and discovered the relationship between roughness and number of laser-passes as illustrated in Fig. 18. It is evident that roughness profile decreased with increased laser passes; this could be because of consistent impact of irradiation from laser beam and rapid vaporization of materials not allowing material to resolidify or cause structural changes on workpiece surface.

Micro cracking is also an issue induced by material properties after laser drilling. Studies [33, 34, 53] found that the cause of micro cracking is because of mechanical properties of workpiece, which is caused by cooling down process. As workpiece cools down, tensile stresses are formed by structural contraction which restricts the material to relax and hence
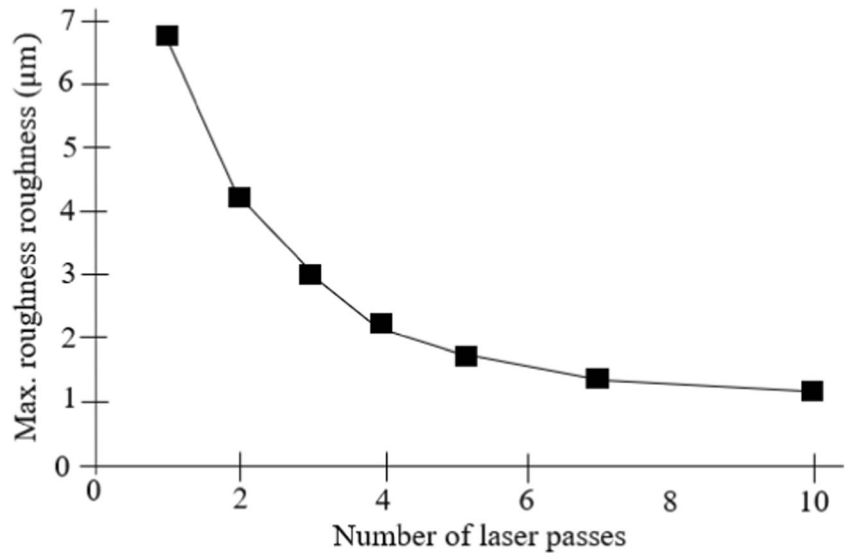
causing micro cracking [53]. An example of micro cracking developed on inner-outmost layer of a drilled hole of Inconel-718 is shown in Fig. 19. However, Wang et al. [48] discovered that by adding localized plasma heating to laser drilling, micro cracking can be decreased by 1.2 times.

Spatter is one of the flaws of laser drilling and it happens when molten material is dispersed round the circumference of hole. It is occurred during initial pulse from laser and is increased mainly with higher energy density of laser beam [34, 54].

5 Electrochemical drilling

Electrochemical drilling is an unconventional drilling process that removes material, which is generally metal, from the workpiece by electrochemical dissolution accordingly to Faraday's law. Electrochemical drilling includes an anode and a cathode that are surrounded by electrolyte. Figure 20 shows a standard

set-up for an electrochemical drilling process, where the tool is directed to the workpiece by Z-axis, the tool and workpiece are both connected to the power source on the negative and positive terminal respectively, and constant electrolyte fed into the system. Lastly, the sludge is removed from the tank through an additional pipe [56]. With adequate potential difference, drilling of the workpiece can then be carried out [55–57]. The electrolyte is driven in between the space of the tool and workpiece, where electric current flows through electrolyte and corrodes the workpiece [58]. Electrochemical drilling process has been advanced to drill materials with high hardness, conductive materials and metals, semiconductors and hybrid materials [55]. Different materials will respond differently to this process due to grain structure and passivation of material [59]. Electrochemical drilling was also established to produce holes with high aspect ratio. Since the process involves the dissolution of material, great quality surface can be obtained on a compound surface. Unlike EDM, ECM process is absent from tool wear and heat affected

Fig. 19 Micro-cracks on the inner surface of a drilled hole on Inconel718 [34]
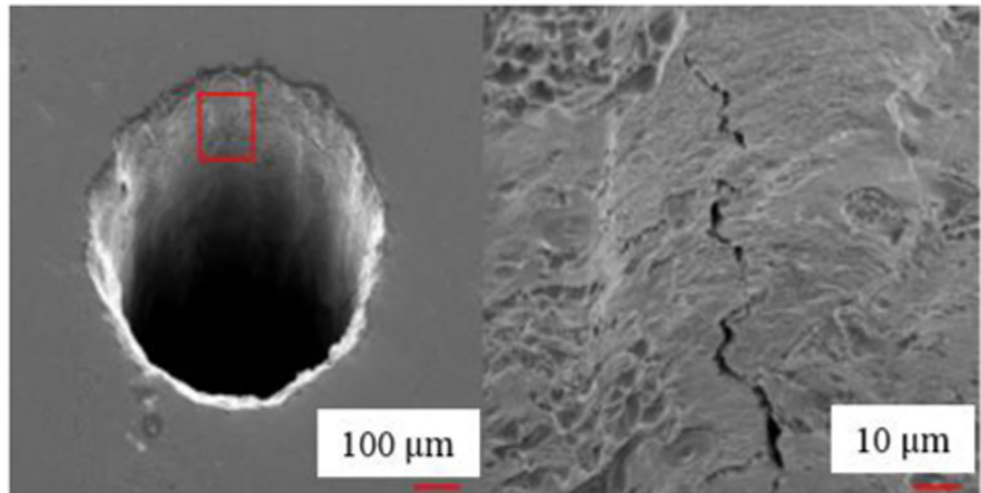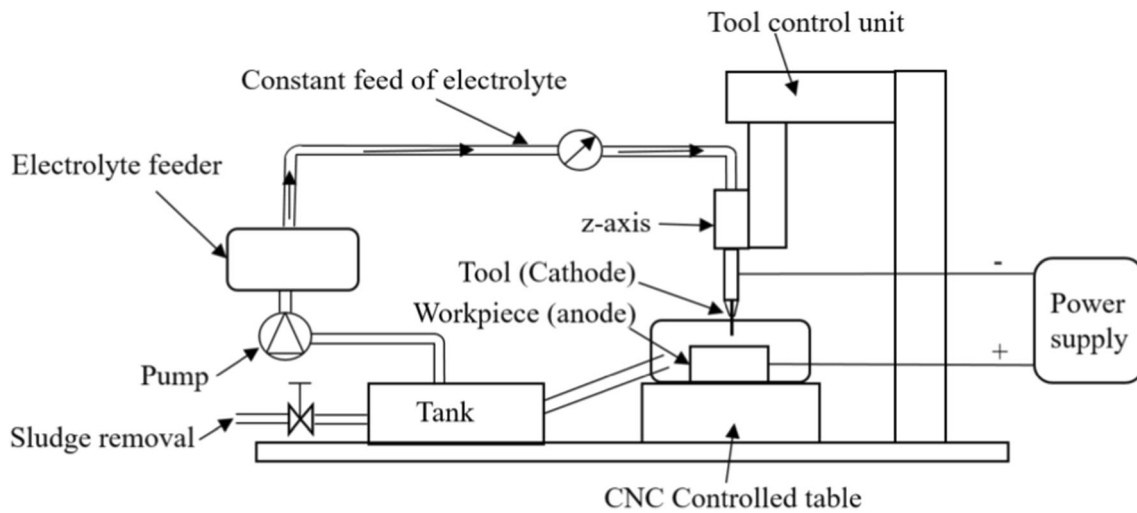
Fig. 20 Schematic diagram of electrochemical drilling [55]

zones [60]. Furthermore, there are many advantages for ECM that makes it unique and they are (i) drilling rates can easily be controlled by electric current, (ii) type of electrolytes that do not harm environment, (iii) absence of heat affected zones and mechanical stresses, (iv) does not alter work piece properties, (v) materials able to withstand chemical reactions such as stainless steel or titanium can be drilled and (vi) able to drill multiple holes at one instance. Besides the difficulty of creating holes lesser than 0.8 mm in diameter, electrochemical drilling generates a good quality surface and is known for high material removal rate [61]. Due to its excellent traits, ECD is widely used in aerospace industries for jet turbine blades, space and automobile industry, electronics industry and many others [9, 62, 63].

5.1 Mechanism

The basic principles of material removal follow Faraday's law where the workpiece is liquefied with adequate amount of voltage being applied between the opening of electrode and substrate that is occupied by electrolyte. The substrate dissolves when the path of electric current flowing through the electrolytic cell is opened (Fig. 21). The ECD process generally utilizes a concentrated salt solution known as electrolyte.

The electrolyte is supplied between the electrode gap at high pressure in order to eliminate reacted materials of workpieces and permit high material dissolution. Figure 22 illustrates material erosion during electrochemical drilling process. The tool used for this process is normally shaped as a tube and the materials commonly used for tools are made of stainless steel, copper or brass [9, 58, 59]. The tool external surface is normally insulated apart from the tip [9]. The tool chosen for drilling should have the following characteristics: (i) excellent mechanical and electrical properties, (ii) adequate stiffness to overcome electrolyte compression, (iii) able to withstand corrosive solutions and (iv) conductor of heat and poses excellent machinability. The choice of tool should be appropriate for the material properties of the workpiece [55].

The type of solution generally favoured for electrolytes are sodium chloride, sodium nitrate, sodium chlorate or a combination of these. The purpose of acidic electrolytes is to corrode and dissolve the workpiece and also used for draining fragments in the form of metal ions from workpiece surface to achieve good surface finish with small tolerances and high aspect ratio holes [9]. The electrolyte also prevents heat from building up in the machining area. In addition, electrolyte creates anodic films on substrate to ease the process [55,
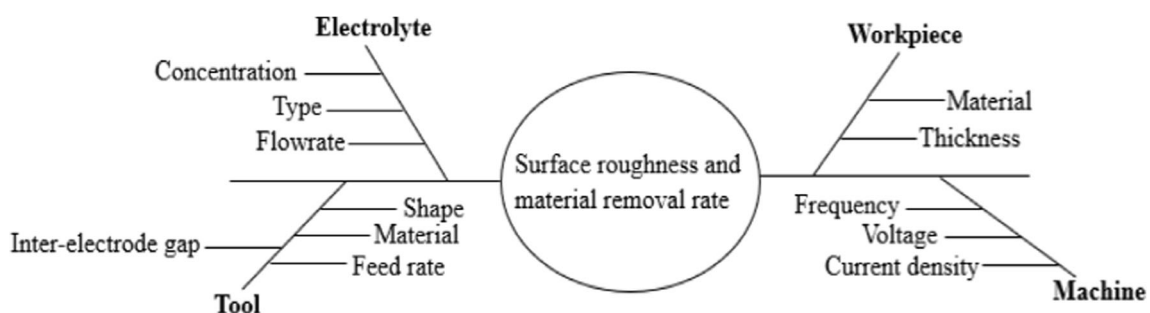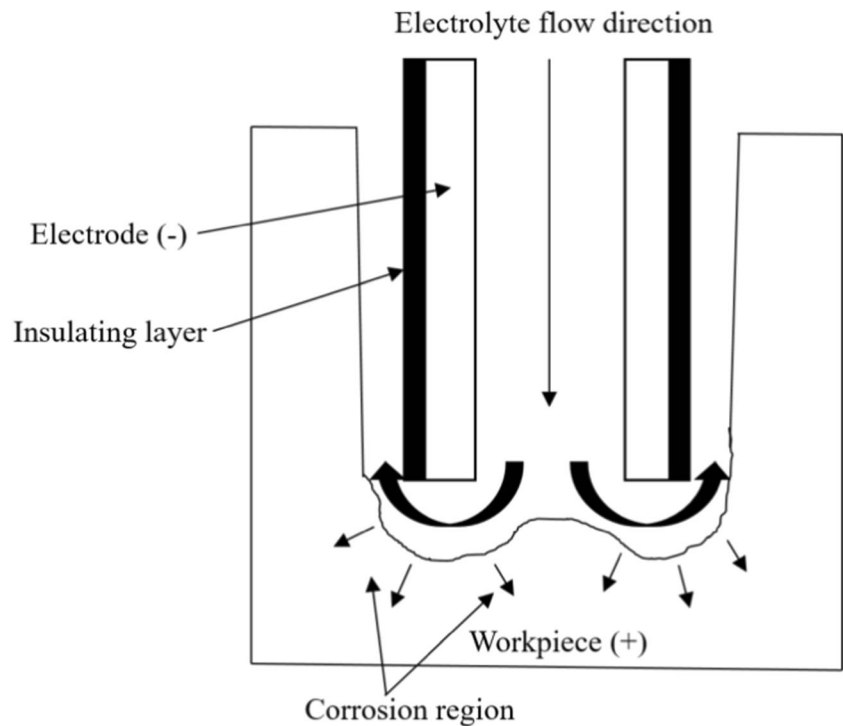

Fig. 21 Factors affecting the quality of hole and drilling rate

Fig. 22 Electrochemical drilling
process [64]

Electrolyte flow direction

Electrode (-)

Insulating layer

Workpiece (+)

Corrosion region

Fig. 22 Electrochemical drilling process [64]

58]. The ions motion in electrolyte is the reason why the current is able to circulate in electrolyte. The ions are charged transporters that create electric field due to the potential difference between the tool and workpiece [64]. The purpose of pulsed electric current is to stimulate the electrolyte to create electrical reaction between the tool and workpiece. In an event of drilling using DC-voltage, used electrolyte will start to boil because of the increase in machining current. As a result, waste products are formed which may stick onto substrate and tool. During this circumstance, further drilling may not be simple. But these difficulties can be tackled by using pulsed voltage in electrochemical drilling. As temperature drops during pulse off time, the waste products will be removed easily. [55].

The drilling performance of electrochemical drilling is controlled by the way the anode reacts in electrolyte. Sharma [58] et al. found that when drilling copper rod on copper strip, electrode colour changes to black. This is due to the composition transformation of the electrolyte. The quality of hole and drilling rate are influenced by the parameters as shown in Fig. 21.

Constant electrolyte flow was implemented by Wang et al. [63] to improve the capabilities of ECD, where continuous feed of electrolyte results in constant refreshment of electrolyte. As drilling depth deepens, electrolyte stream will get clogged easily [9]. The heat that is formed in drilling process will build up around drilling region. These issues will disrupt electrolyte flow and with time, drilling will have to come to a halt due to short circuit or the machining process will not be suitable to carry on. Hence, large holes cannot be drilled if the

replenishment of electrolyte is inadequate. Hence the importance of constant refreshment of electrolytes is essential [63].

5.2 Material removal rate

Material removal rate is defined as the feed rate that governs the current flow between anode and cathode. As the tool descends closer to workpiece, the gap narrows and the current increases; hence, raising material removal rate. Material removal rate is proportional to voltage, electrolyte concentration and temperature [65–67]. Figure 21 shows the various parameters affecting the surface roughness and material removal rate. Several studies found that major parameters influencing MRR are the concentration and type of electrolyte, current density, applied frequency and feed rate.

Manikandan et al. [56] used titanium alloy as workpiece with sodium nitrate as electrolyte. The main parameters affecting MMR in this study are feed rate and electrolyte concentration. The results show these two parameters are directly proportional to MRR. The trends can be found in Figs. 23. MRR increases due to increase of feed rate as when the electrode reaches closer to the workpiece, higher volume of negative ions transfers to electrode and removed by electrolyte. This will stop happening if feed rate gets too high till the contact between the electrode and substrate lead to short circuits. The reason why MRR increases when feed rate increases from 0.15 to 0.2 is because in this range, voltage in the interior space of the electrode is sufficient enough to remove the material from substrate. It was shown that MRR increases with electrolyte concentration as electrolyte solution strength increases, electrochemical reaction between the
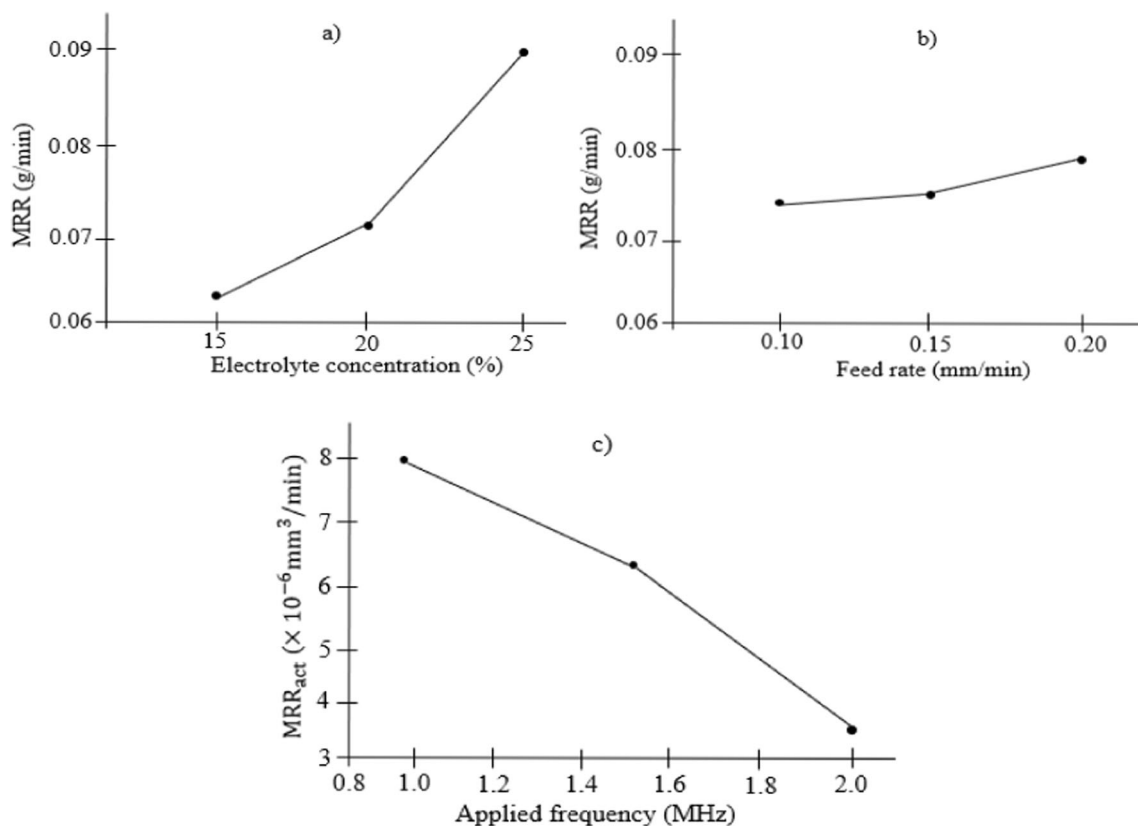
Fig. 23 Relationship between the **a** concentration of electrolyte, **b** feed rate and **c** applied frequency on MRR [56, 68]

workpiece and electrolyte increases; hence, the rate at which the ions are carried away by the electrolyte flow increases, which increases MRR [56]. A similar result was found by Manna and Malik [69] where MMR increased with higher concentration of electrolyte. Rao [70] et al. obtained similar results by using Taguchi methods and ANOVA for optimization of the parameters affecting MRR and found that feed rate and concentration level of electrolyte are directly proportional to MRR.

MMR depends on faradaic current, whereby an increase in current increases MRR as increase in ions took place in the middle of inter-electrode gap which increases the dissolution of workpiece [71]. Goswami [72] performed ECM on mild steel and aluminium and also reported that current affects MRR and surface roughness. In this study, the frequency effect on MRR was investigated and the results show that MMR decreases when the applied frequency increases. The trend can be observed in Fig. 23 [68]. Another study also [73] reported similar results where MRR decreases with higher frequency. This is because with higher applied frequency, current density decreases which results in low MRR.

Da Silva [74] et al. reported that process temperature is proportional to MRR as the conductivity of electrolyte changes with temperature, and that the higher the temperature, the faster is electrolyte evaporation. Hence, the temperature of electrolyte is normally maintained roughly between 25 and 60 °C. It was found in this study [3] that machining rate was

faster when drilled with rotating edge-cut electrode as compared with rotating cylindrical electrode. This is possibly due to the increase in surface area on the bottom of tool tip that contributes to a larger amount of material removed, thus increasing machining speed.

5.3 Hole characteristics and surface finish

Hole quality and surface roughness are generally influenced by factors like pulse current, frequency, inter-electrode gap, type and tool shape, flow rate of electrolyte and of course the concentration of electrolyte. Common types of circular hole features achieved from electrochemical drilling are overcut, aspect ratio and hole taper. Overcut is defined as half the size after deducting hole diameter from tool diameter. Taper angle can be measured using hole entrance diameter and the size of the exit of holes [55].

Sen and Shan [9] experimented on the difference of a dual pole tool and an insulated tool, and reported that when using the dual pole tool, stray removal at the interior side surface of hole and hole taper decreases. The drilling reliability and precision increase when using dual pole tool. An example of the difference in both tools is shown in the graph in Fig. 24.

One of the greatest issues faced in ECD is the formation of taper. Taper angle for blind hole is normally greater than through hole. This is firstly, it is not easy for the electrolyte
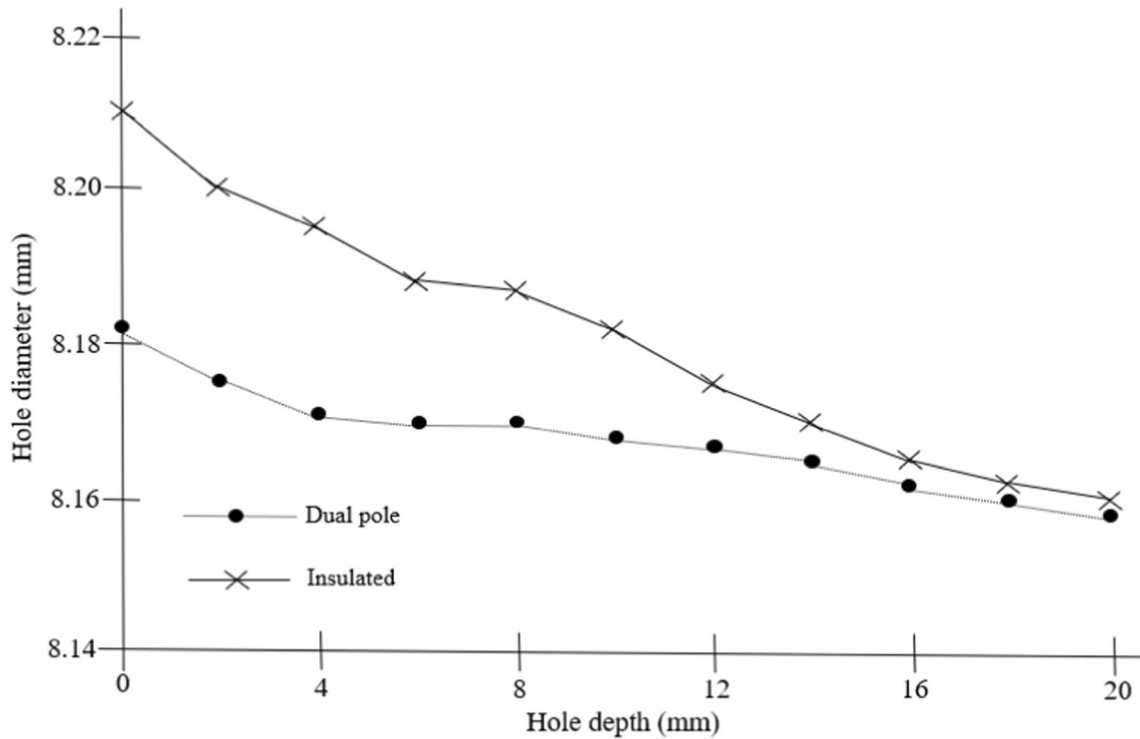
Fig. 24 Comparison between dual pole and single insulated pole [75]

to penetrate deep into hole as is difficult to dissolute the metal. The second reason is due to boiling of electrolyte; bubbles are formed that are stuck in small machining opening which raises the resistance against dissolve of subtract. This will then cause the current to flow from the side to entrance of the hole which will cause the hole to be enlarged. The third reason is due to chemical reaction to dissolve subtract. As during that process, chromium oxide layer is developed which will then stop the dissolution process. Lastly, taper is created because of the gap in between the drilling time in the middle of both top and bottom hole, as taper reduces as tool feeds through the holes [60]. A study conducted in [59] by Chryssolouris et al. found that hole taper and overcutting increased, when voltage and concentration of electrolyte increased. This is possibly due to rise in the number of ions present in the solution as concentration of electrolyte increases; which then increases the amount of material removed at the top hole and thus the hole taper is increased. The increase in voltage would increase electric current density and hence, speed up material removal process at top hole.

Manikandan [56] et al. found that when feed rate increases, the overcut increases as shown in Fig. 25. The reason why there is no change between 0.15 and 0.2 mm/min is because as electrode moves at high rate; MMR at lateral direction is not as effective as when it moves at a low speed. Hence the overcut is larger between feed rate range of 0.1–0.15 mm/min. Manikandan et al. also reported that electrolyte flow rate is inversely proportional to overcut as rise in electrolyte flow

rate results in decreasing the flow of ions from substrate in lateral direction. The overcut is also inversely proportional to electrolyte concentration [56].

The type of tool used affects the quality of hole achieved. Figure 26 shows different type of holes drilled by different tools: (a) a flat bottom tool was feed, and the middle section of the hole was not eroded; and (b) a rotating edge-cutting tool was used. This was because when using flat-ended tool, supply of electrolyte solution was irregular [55]. Wang [63] et al. found that flow rate is proportional to circularity and hole quality. The effect of circularity of hole with flow rate and constant pressure is shown in Fig. 27. Under constant flow
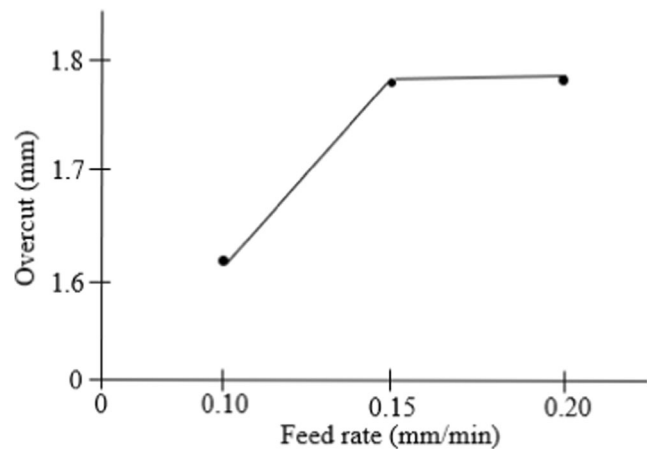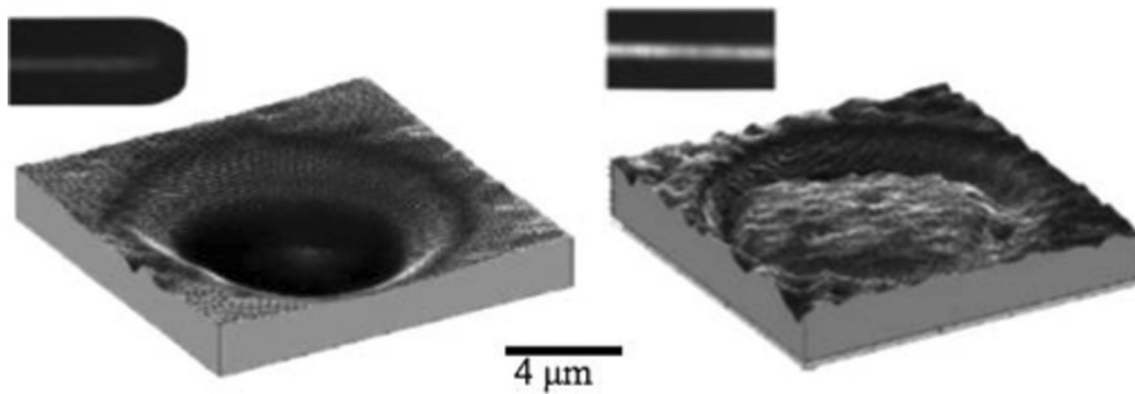

Fig. 25 Feed rate influence on mean overcut [56]

Fig. 26 Morphology of hole surface formed by using different shaped tools (Ø 4 μm) [60]
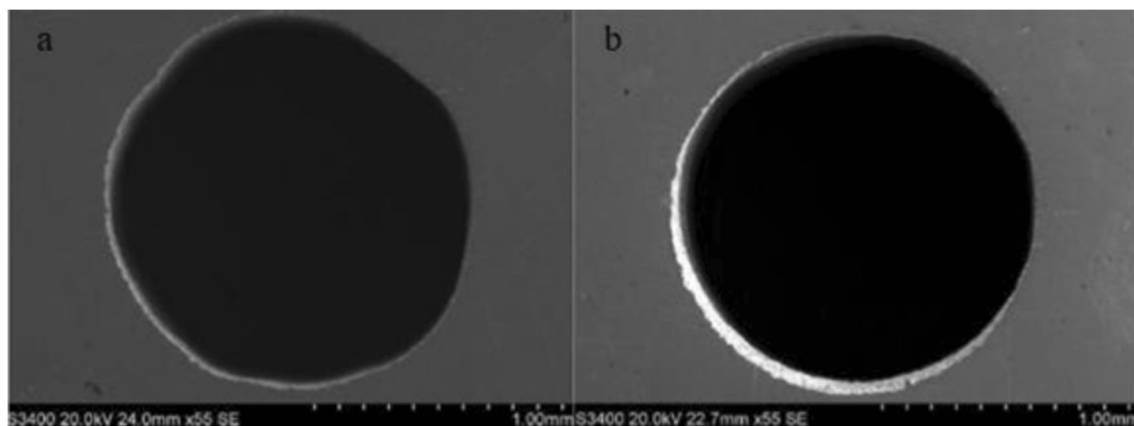
rate, hole circularity is a little out of shape because of insufficient electrolyte to wash away the fragments. In addition, heat accumulated from hole depth as pressure decreases during the flow which disrupts the flow rate and conductivity of electrolyte. Additionally with higher electrolyte flow rate, higher rate of waste products disposal enhance hole circularity [63].

To obtain good surface quality and smooth surface, ECM performance can be enhanced by reducing pulse current [55]. A similar study conducted by Qu et al. [76] also found that surface roughness increases with pulse current. During pulse off time, it gives time for the electrolyte to wash away any waste products on workpiece and also the heat produced due to the effect from inter-electrode spacing. Hence, surface quality can be improved. Figure 28 illustrates the relationship between pulse amplitude and surface roughness.

6 Electro discharge drilling

Electro discharge drilling (EDD) is a process which includes a combination effect of thermal and electrical operations. Holes are normally achieved when electrical energy is being used to create sparks which produces thermal energy to remove materials. The space in between two electrodes placed close to

each other, which creates a spark in a dielectric solution. The potential difference applied between the electrodes is significantly high. Hence at that particular zone, temperature is high enough causing ablation of the material [2, 77]. Figure 29 shows the schematic diagram of EDD system, where both tool and the workpiece are connected to the power source to negative and positive side of power supply, respectively. The tool is controlled by controller and dielectric feeder constantly feeds drilling zone with dielectric. According to Lim et al. [79], the cost of set-up of micro EDD machine is low where non-contact feature needs less force between electrode and workpiece to drill hard and brittle material. The non-contact process for EDD makes it advantageous as compared to conventional machining as it eliminates any mechanical stresses that occur during machining processes. However, pitfall of this technique is that materials have to be electrically conductive regardless of its hardness [80]. Furthermore, speed at which material is removed from workpiece is lower than other non-traditional techniques and the tool experiences wear [1]. Hence longer electrode or constant replacement of electrode will be needed to improve drilling efficiency. Micro-EDD drilling is believed to be an efficient method for creating holes in micro-components as compared to other unconventional drilling methods. EDD is also known for fabricating

Fig. 27 Entrance drilled hole on Inconel 718 under different flow rate: **a** 140 and **b** 245 ml/min [63]
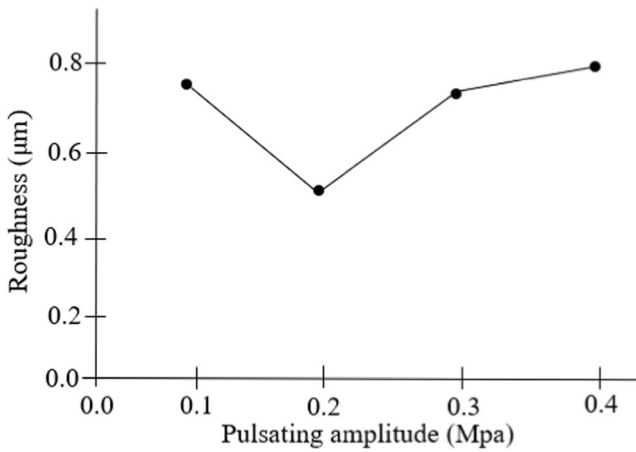
Fig. 28 Relationship between pulse current and surface roughness [76]

as an insulator and prevents electrolysis during drilling process. Discharge energy is produced from the voltage in power supply overpowering the dielectric degradation over small space. At this stage, plasma is generated, and temperature can rise up to 20,000 °C. Thermal energy from sparks melt and evaporate the substrate as well as wear in electrode took place due to material removal. After sparks are produced, plasma channel breaks down and hence the pressure acting on the surface of the crater reduces. Material removal process occurs in spark zone which is a complex process in EDM and consists of several physical procedures. Removal of the eroded workpiece can be expelled in two ways: (i) through ablation and (ii) bubble explosion. After evaporated materials cools down, it forms debris that are flushed out by dielectric fluid [82–85]. An illustration of the drilling process is shown in Fig. 30.

A number of papers [86–88] that carried out different experiments have reported that there are factors that affect the efficiency of micro EDD process. Those parameters are voltage, pulse duration, peak current, spark gap and system parameters such as properties of the tool, dielectric fluid as well as physical and chemical properties of workpiece. Different types of dielectrics influence the performance of EDD drilling due to various chemical compositions, viscosity, strength and cooling rates [86]. Because of difference in viscosity, behaviour of flushing is affected. As boiling temperature for hydrocarbon oil is comparatively higher than water-based dielectrics, this influences in more discharge energies and increase discharge duration. In water-based dielectrics, breakdown strength in electrode gap is large hence improving flushing and better cooling conditions as

complicated shapes and moulds for the moulding industry. EDD is commonly used in aerospace and automobile companies on turbine blades and injection nozzles [81].
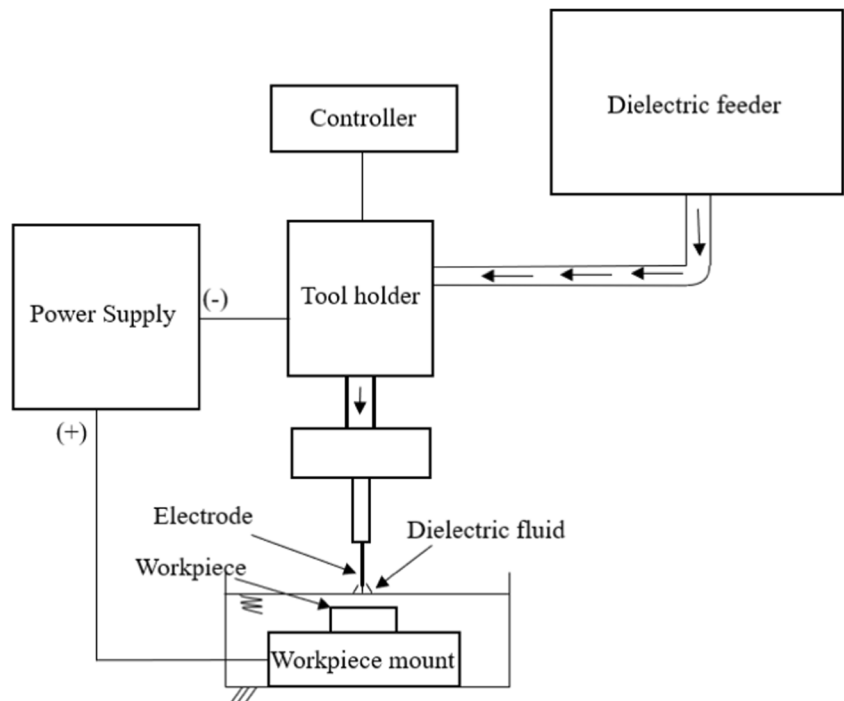
6.1 Mechanism

The stages of material removal from EDD can be summarized into three stages: (i) melting of material, (ii) evaporation of material and (iii) washed away by a suitable dielectric fluid. EDD is a mixture of both thermal and electric process where the erosion of the workpiece is due to high energy discharged from electricity. Drilling of holes by EDD is possible because of the spark produced when electrode is close to the workpiece. Sparks normally occur in a dielectric medium which act

Fig. 29 Schematic diagram of electro discharge drilling [78]

**Fig. 30** Electro discharge drilling process illustration
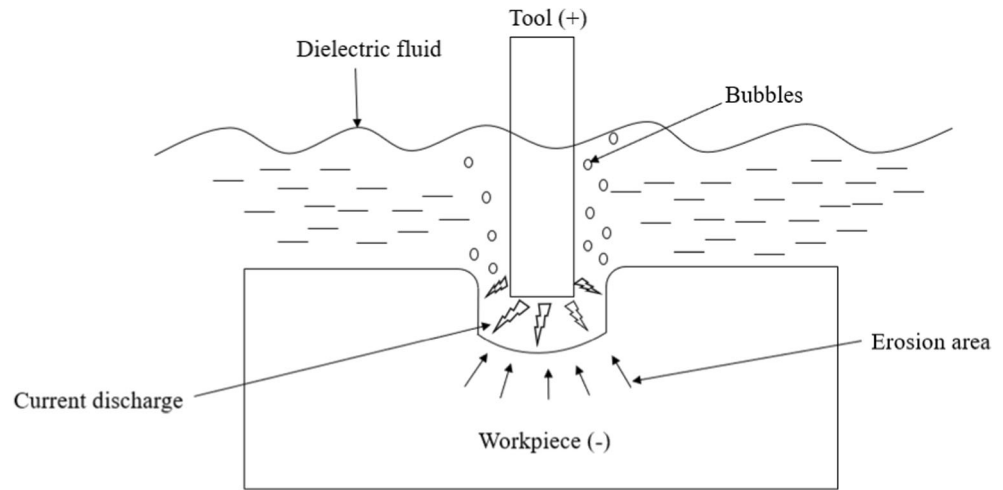
compared with hydrocarbon oil [88]. Jilani and Pandey [87] reported that for metal removal rate, tap water was a better option than distilled water and on contrary, electrode wear on brass tools were higher when using tap water as compared to distilled water. Hole quality and drilling rates are dependent on the factors shown in Fig. 31.
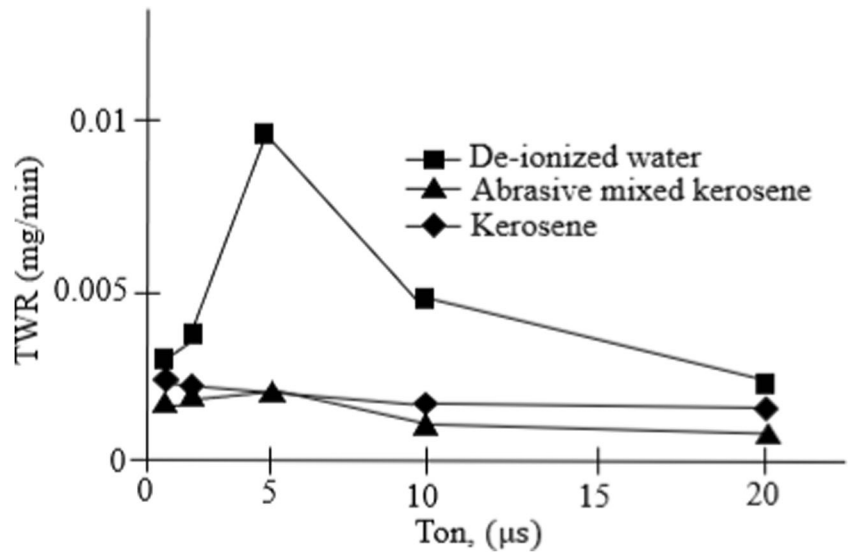
6.2 Tool wear

Electrode wear contributes towards the irregularity of holes achieved by micro EDD. As the electrode continues to drill into workpiece, severe wear will occur on electrode as compared to other parts. It has been investigated that micro EDD is able to generate features that are less than 5 μm in dimension with surface roughness lower than 0.1 μm. During micro EDD, electrode implants into material and hence erosion of electrode occurs massively [89]. The electrode's bottom end wears at initial stage of drilling followed by the edge of the electrode. Carbon oil reduces tool wear after a certain period as carbon itself started to form a protective layer on electrode surface which helps the prevention of additional tool wear [89].

Electrode wear occurs mainly on side and bottom end of electrode, where bottom wear affects the length of electrode and side wear affects hole accuracy, which cannot be disregarded in most occasions [77]. Major parameters such as voltage, current, pulse time, material properties and types of dielectric uses should be understood before executing drilling process. Different workpieces such as tool steel, brass and aluminium were examined to see if tool wear varies with different materials. The electrode material used was tungsten carbide. The result concluded that for soft materials like aluminium and brass, tool wear rate was lower as compared with tool steel as melting points for tool steel is much higher compared to aluminium and brass and hence, material removal for brass and aluminium is easier. In addition, smaller grain size of workpiece material forms smaller debris and hence, higher wear occurs on tool when drilling tool steel [77]. The results also showed that tool wear rate was higher after using deionized water as compared with kerosene as decomposition of kerosene occurs when heated up to a certain temperature and hence, gives out carbon particles that bond with the surface of electrode surface and hence preventing rapid tool wear during drilling process [86].
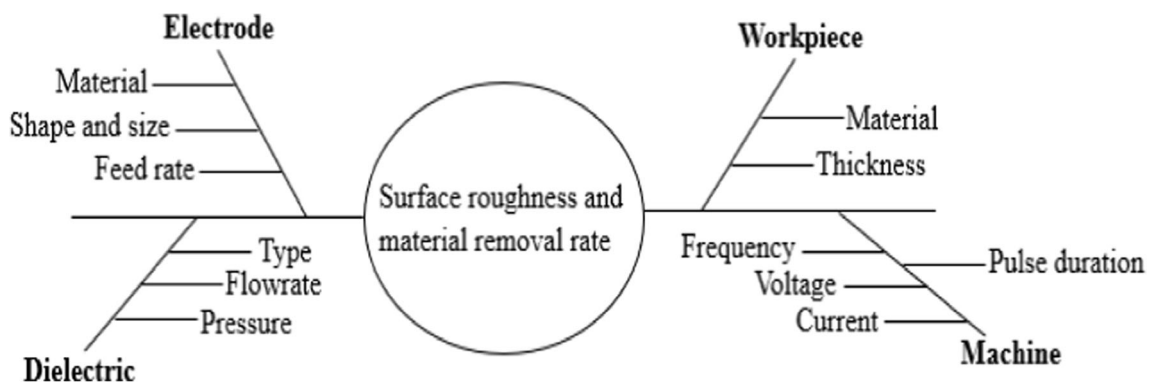
Fig. 31 Parameters influencing the surface roughness and material removal rate during EDD

Kibria [86] et al. reported that tool wear, when using de-ionized water as dielectric fluid, was highest when compared with kerosene and kerosene mixture with abrasive particles. The trend can be observed in Fig. 32 and the reason why deionized water contributes to a higher tool wear rate is at high temperatures, degradation of kerosene occurs, and carbon is produced as a result. Carbon particles will then stick onto tool surface and act as a protective layer against erosion, hence tool wear is lower. However, carbon is not released by deionized water during the process and hence no defensive layer will be created on tool. In addition, burning happens more in drilling area which results in higher wear when using deionized water as dielectric.
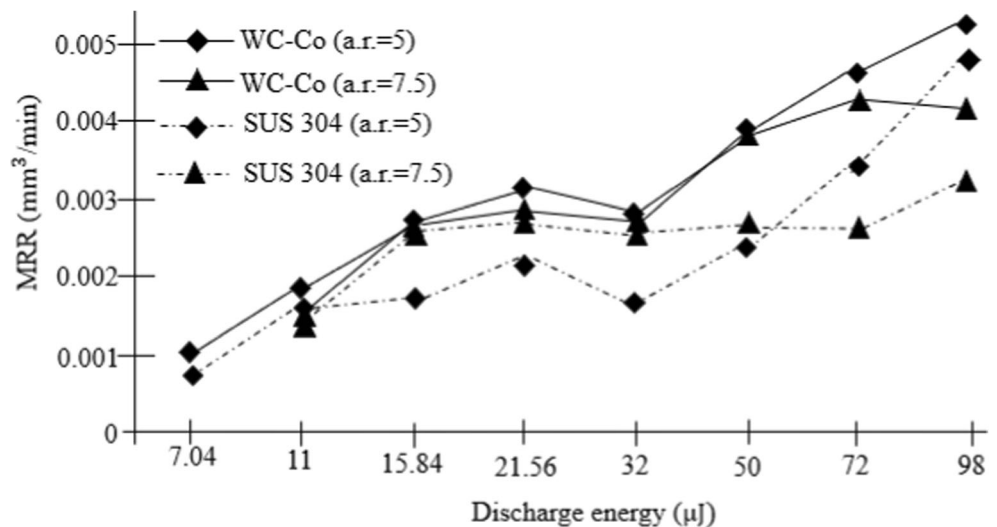
6.3 Material removal rate

Generally, material removal rate (MRR) is the most essential target during EDD. MRR of two different types of electrodes were investigated by Yilmaz et al. [78]. Single-channel and multi-channel electrodes made of copper and brass were studied. Highest MRR recorded was from an individual channel brass electrode. The single-channel copper electrode was found to have a higher MRR than multi-channel electrode of both brass and copper. Hence it is obvious that single-channel electrode is superior as compared to multi-channel electrode. The reason why multi-channel has a lower material removal rate is mainly because of the flushing process which is also known as cooling process. It is common that excessive cleaning of the gap decreases expelled frequency due to rapid replenishment of insulation. The outcome of this is that melting of material due from generated heat is lowered and hence, lesser material is eroded from workpiece and washed away [78].

The rate at which material is removed when using brass electrode is higher than tungsten carbide electrode as electrical conductivity seems to be significantly higher for brass

Fig. 33 Relationship between discharge energy and MRR for different materials [90]

**Fig. 34** Type of dielectric's influence on material removal rate [86]
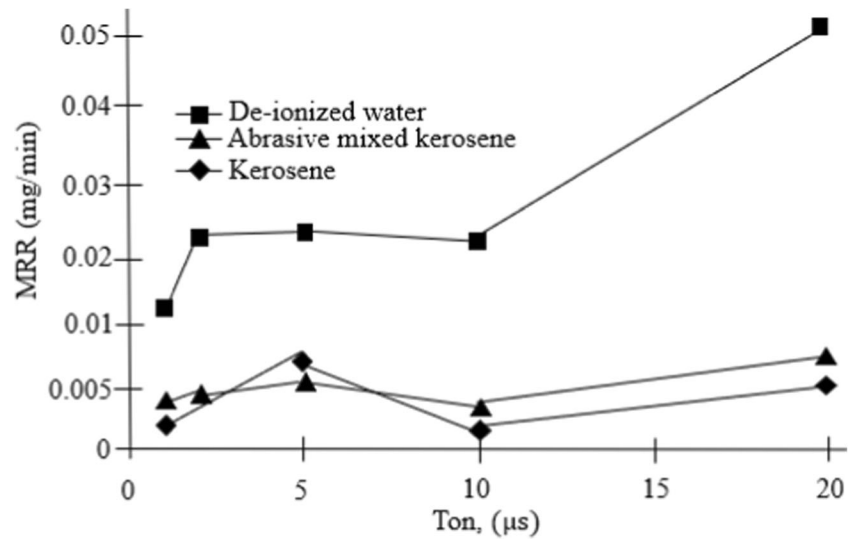
electrode [85]. Jahan et al. [90] reported that electrical resistivity of both materials affects MRR. Electrical resistivity for SUS 304 is significantly higher than WC-Co. As electrical resistance is high, this limits the conversion of material energy from electrical to thermal, hence melting and evaporation action decreases. Figure 33 shows material removal rate of both materials and it can be observed that material removal rate varies with different material corresponding with same discharge energy and for this case, MRR rate for WC-Co is higher than SUS 304 [90]. Similar results were reported by Yilmaz et al. [78] who used titanium alloy and Inconel 718 as workpiece and wanted to find out the variance in MRR. They reported that material is removed at a faster rate from Inconel 718 than titanium, due to the higher electrical resistivity of titanium alloy [78].

Kibria et al. [86] investigated the influence of dielectric fluid on material removal rate on titanium alloy and reported that when deionized water is used, material was removed faster than when pure kerosene was used. This is due to formation of oxide (TiO_2) layer that developed on the outer surface of workpiece that melts on low discharge energy as compared with melting of carbide (TiC) created due to kerosene. Furthermore, deionized water can act as a mild electrolyte which assists in removing larger amount of material as shown in Fig. 34. Boron carbide powder was mixed with kerosene to be used as abrasives and the MRR rate improved slightly as boron carbide particles assist kerosene by producing even supply of discharge energy and improve electrical conductivity which results higher machining performance. Various studies [85, 91, 92] also agree that MRR increases with higher discharge current as shown in Fig. 35. The reason is, at higher current, spark energy created between electrode and workpiece gap is large, hence material removal is higher [92].

Fig. 35 Influence of discharge current on material removal rate with different electrode speed [92]
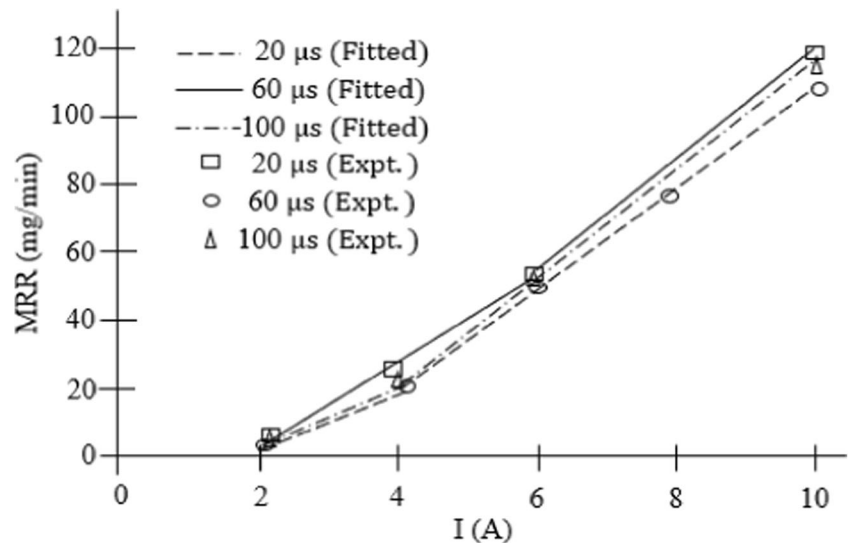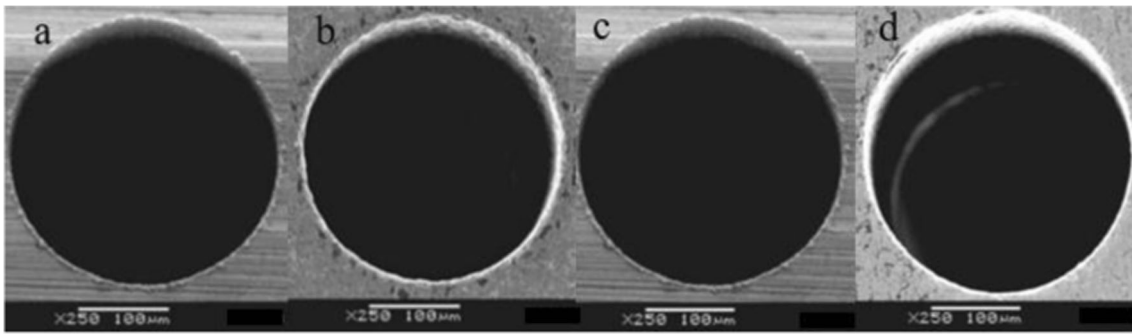
Fig. 36 Effect of discharge energy (DE) and aspect ratio (AR) on hole quality: **a** DE = 7.04 μJ and AR = 5 on WC-Co, **b** DE = 7.04 μJ and AR = 5 on SUS 304, **c** DE = 11 μJ and AR = 7.5 on WC-Co and **d** DE = 11 μJ and AR = 7.5 on SUS 304 [90]

## 6.4 Hole characteristics and surface roughness

Hole circularity, accuracy and smooth surface are desired by the manufacturers. Studies have revealed that significant factors such as discharge energy, workpiece properties and electrode type influences the characteristics of holes formed by machining. A study conducted by Jahan et al. [90] shows the effects of workpiece material properties and discharge energy as shown on Fig. 36 on both cemented carbide (WC-Co) and stainless steel (SUS 304) workpiece. As it can be seen with the increase of aspect ratio and discharge energy, size of holes increases. However, with same aspect ratio and discharge energy, it can be seen that hole size for SUS 304 expands more at the top hole. Overcuts produced on SUS 304 are greater as well, hence the accuracy of holes are reduced. However, for WC-Co, it can be seen that the hole created expanded lower than SUS 304 at the absent of burrs and slightly affected by heat. Debris found on hole surface on SUS 304 are not burrs but they are the excessive amount of carbon released from dielectric oil that increases after drilling process and solidifies on the rim of hole. The quality of surface at the rim of WC-Co is good enough [90]. This can be explained as WC-Co is a higher conductor of heat than SUS 304, hence lower expansion of holes was realized. It was also found that taper hole was directly proportional to e hole taper as with higher discharge energy, size of the crater on workpiece enlarges and as a result, accumulate and induces sparks occur rarely. Hence, it will be difficult for dielectric to wash away accumulated removed materials which then cause the top hole to be larger than bottom [93]. Another possible reason is that, during drilling process, fragments removed from workpiece travels from the exit to hole entrance, which as a result generate secondary sparks and cause larger hole at hole entrance [94].

D'Urso et al. [85] investigated the influence of discharge energy and electrode material on hole surface quality of AISI 304 as presented in Fig. 37. The energy is the product of peak current and voltage. The higher the energy, the larger is the diameter of the drilled hole. When using brass electrode, reason for the difference in texture of holes and burr like formation is because of solidified melted material [85]. A similar study was done by Ay et al. [80] where higher discharge energy resulted in burr-like formation on the circumference of holes. The reason for that is because of aggressive sparks caused with higher energy and cooling down process after drilling where residues are formed. Figure 38 shows the entrance hole variance from low discharge energy to high discharge energy drilled on Inconel 718. From the figure, heat-affected zone on hole appears under high discharge energy and forms around the circumference of hole. Yilmaz and Okka [78] also reported that heat-affected zone occurs on the circumference of hole and mainly because of high level of discharge energy. Heat-affected zone occurs over various thicknesses of workpiece depending on materials' properties and machining conditions. Yilmaz et al. [78] also found that EDD drilling produces a small round particle of a substance on surface, pockmarks and melted drops. Surface finish for multi-channel brass electrode is better than single-channel
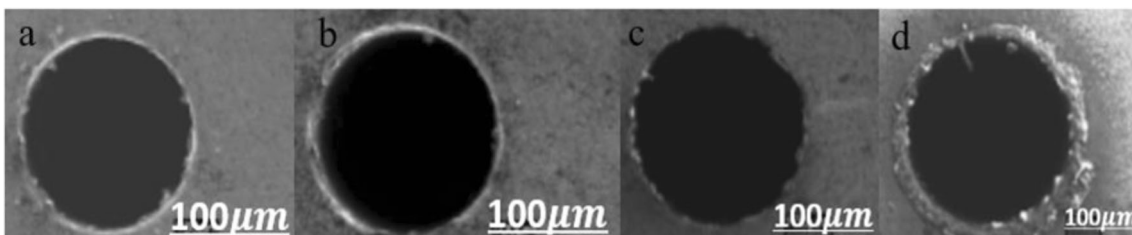
Fig. 37 The entrance of drilled holes on AISI 304: **a, b** using tungsten carbide electrode, **c, d** by brass electrode, **a, c** drilled under low energy and **b, d** drilled under high energy [85]
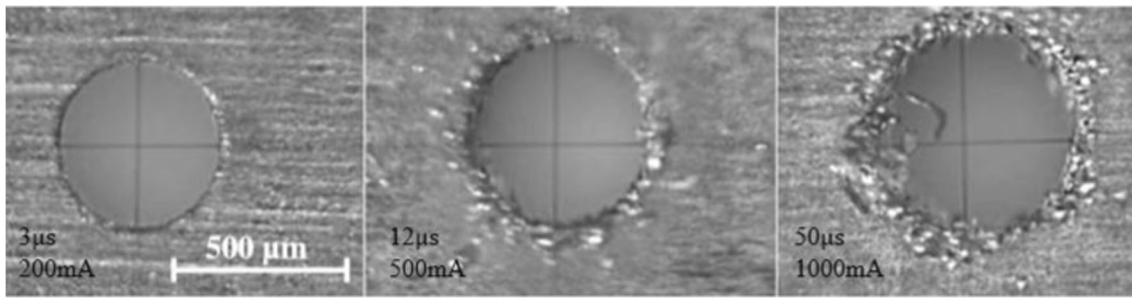
Fig. 38 Increasing effect of discharge current and pulse duration on hole quality [80]

brass electrode as flushing effect of multi-channel brass electrode is stronger and aids the removal of molten or small particles without instant re-solidification.

Kibria et al. [86] found that recast layer on workpiece surface is lesser when using abrasive mixed dielectrics as abrasive removes solidified fragments by friction on workpiece. Lower overcut of hole was found in deionized water as dielectric in comparison to kerosene dielectric at low discharge energy. However, higher overcut was produced when deionized water was used as dielectric under high energy. This is due to larger degradation of deionized water at high temperatures due to high energy where deionized water produces oxygen and hence, assist spark to increase overcut compared with kerosene where no oxygen is produced to assist spark. At low discharge energy, machining effect is slower on inner wall surface of hole when using kerosene which results in higher contact to secondary sparking and hence, overcut will be larger with deionized water as dielectric [86].

Kuppan [92] et al. reported that an increase in either current or pulse would increase surface roughness of drilled holes. The reason is because, as pulse-on time increase, spark density becomes more concentrated and hence, increasing the depth of boundary which will raise roughness value [95]. The reason for roughness increases with current is because, with higher current produced from machine, spark energy increases which then raises discharge power. Therefore, increasing the size of crater and roughness.

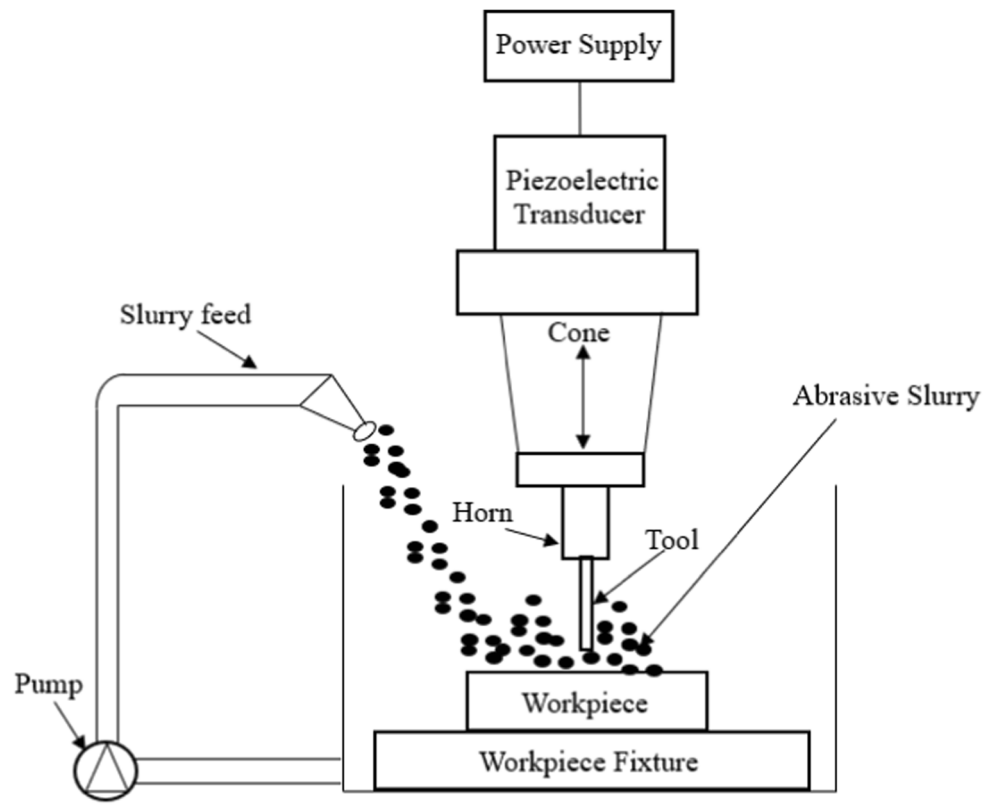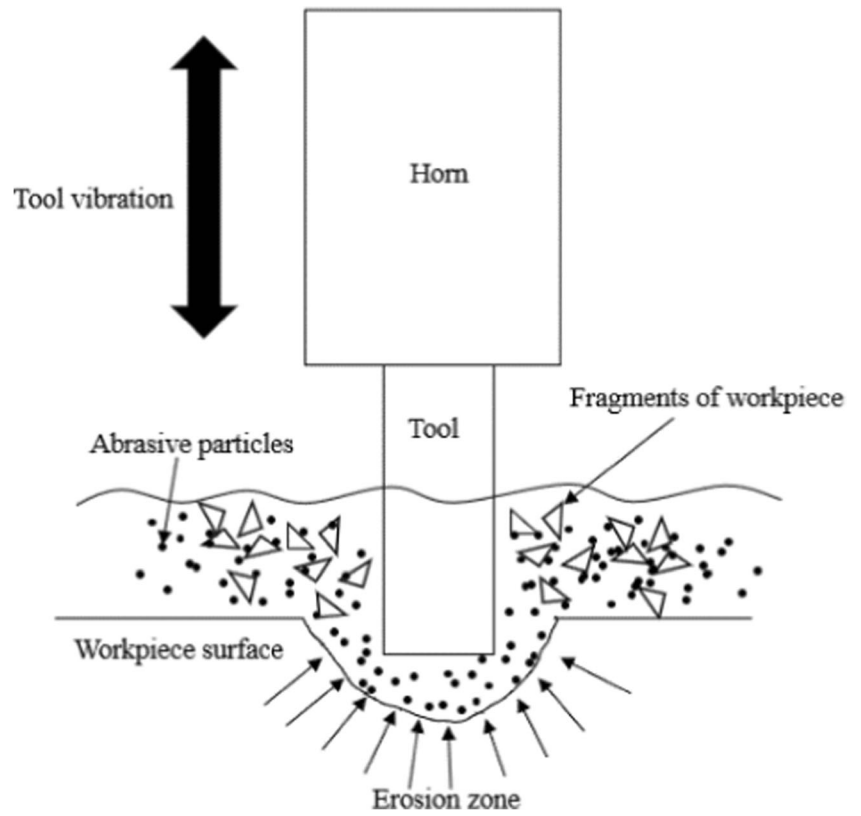**Fig. 39** Schematic diagram of ultrasonic drilling [102]

Fig. 40 Illustration of ultrasonic
drilling process

7 Ultrasonic drilling

Ultrasonic drilling (USD) is a non-conventional drilling process, and unlike EDM or ECM, this process can be used to drill materials that are non-conductor as well as low ductility and hardness [96, 97]. However, compared with EDM and ECM, if tool wear is required to be reduced such as drilling of hard steels, EDM and ECM would be a better option [98]. This process does not cause chemical effects, thermal effects or metallurgical effects on workpiece. Ultrasonic drilling is a mechanical process that does not form recast layer, absence

of cracks and straight profiled holes can be achieved [99]. In USD, electrical energy is transformed into mechanical vibrations which are transferred over to the tool [6]. As a result, tool vibrates at high frequency along linear axis, normally in the range of 20 kHz and amplitude vary from 5 to 50 μm. Power consumption normally lies between 50 and 3000 W. USD produces a static load and vibration to tool together with abrasive slurry. Abrasive fluid mixture contains particles like silicon carbide and boron carbide that are released by either water or oil and fed in drilling area. Tool vibration excites the abrasive particles in liquid carrier
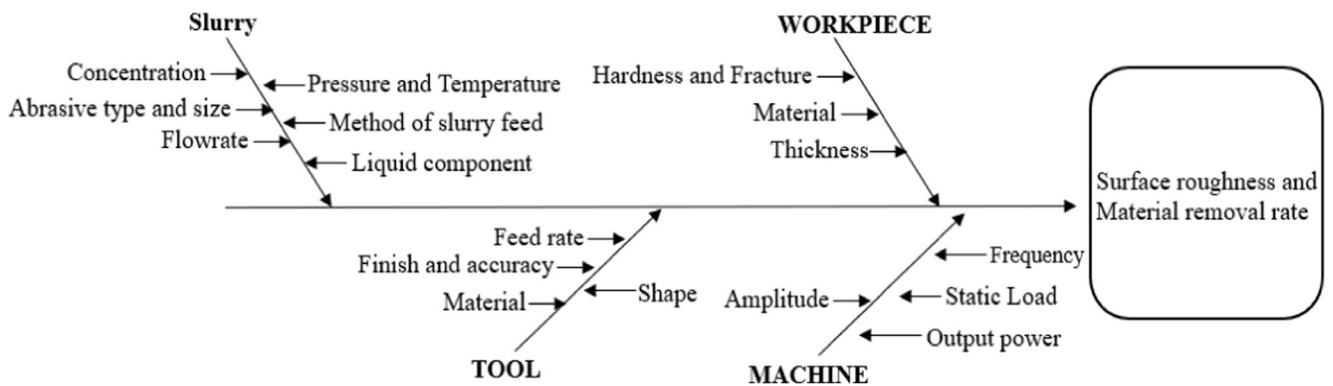
Fig. 41 Parameters influencing hole quality and drilling speed during ultrasonic drilling [99]

Fig. 42 Effect of abrasive and tool materials on tool wear [105]
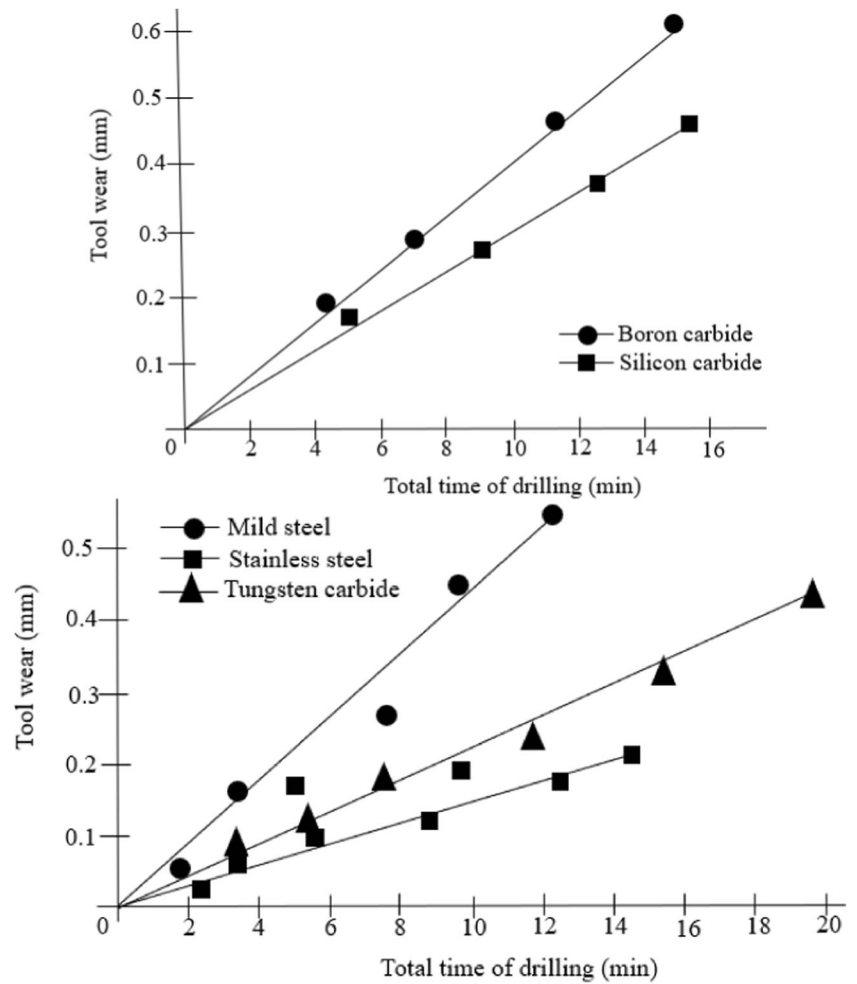
that flows under the tool and on substrate, to strike the top layer of workpiece and erode workpiece by microchipping. According to Moreland et al. [100], hole dimensions as small as 76 μm can be achieved using ultrasonic drilling process but depth to diameter ratio can only be achieved up to 3:1 [101].

Fig. 43 Workpiece materials' influence on tool wear [109]
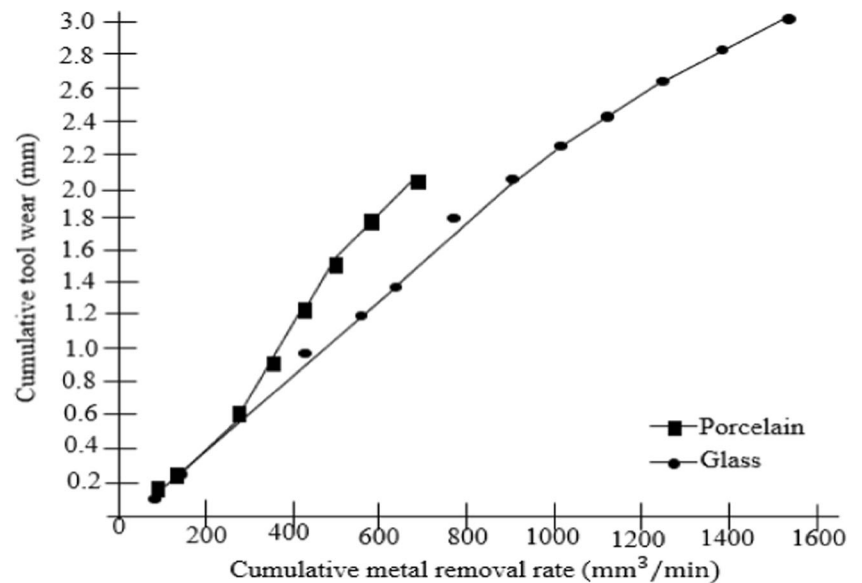
Fig. 44 Influence of abrasive particle size on drilling rate [113]

7.1 Mechanism

Drilling mechanism of ultrasonic drilling can be divided into three stages: (i) mechanical erosion from direct impact of abrasive particles in liquid carrier on substrate, (ii) abrasion due to impinging force by abrasive particles and (iii) removal of material from substrate due to cavitation caused by slurry filled with abrasive particles [6]. Due to the presence of impinging force of abrasive particle on workpiece surface, fractures occur on hard and brittle like ceramics. Power supply stimulates piezoelectric transducer as shown in Fig.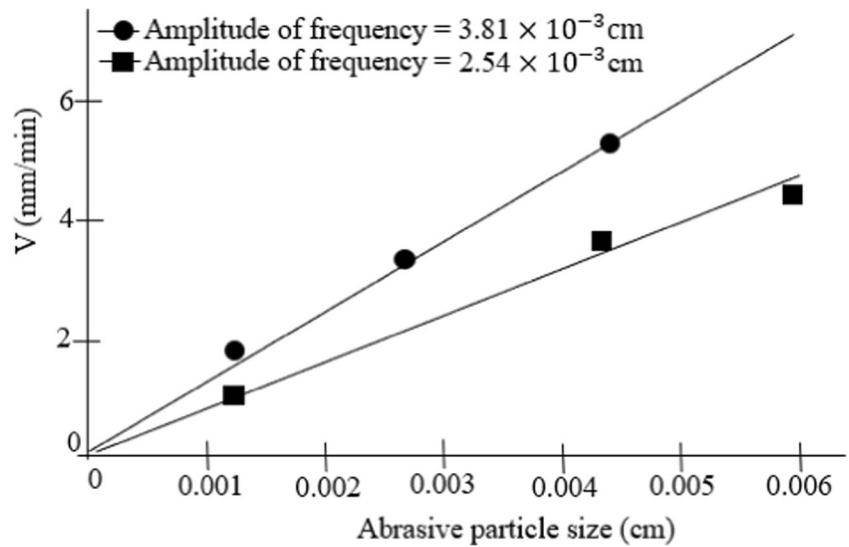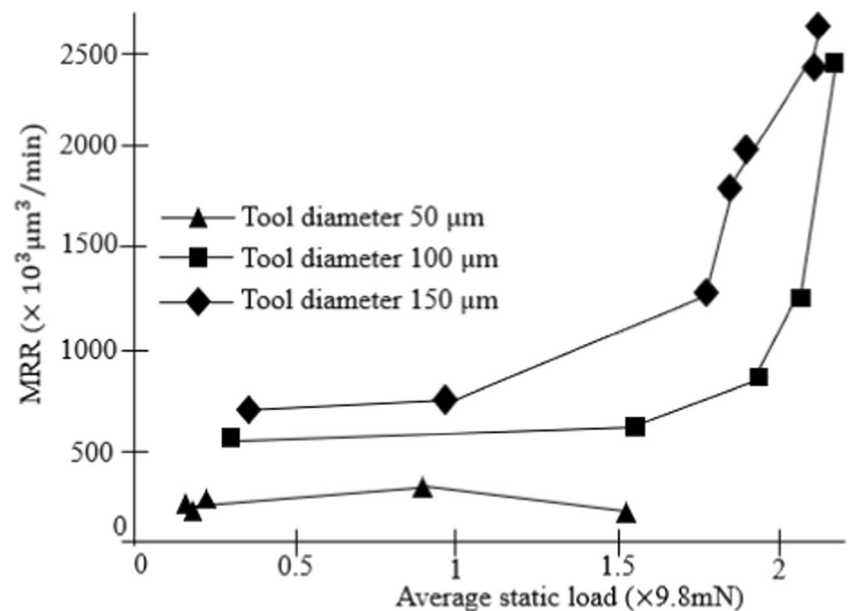 39 which is attached to the horn and drives the tool at a high frequency. The tool then impinges onto substrate which is covered with abrasive slurry. Abrasive slurry will then erode workpiece and create a negative image of the

tool onto workpiece. Hence, profile of the workpiece relies mainly on geometrical tool profile [103]. The purpose of USD is to erode the top layer of workpiece in first stage. Development of cracks on workpiece is governed by mechanical characteristics of the material, original condition of workpiece and the magnitude of static load. The mechanisms discussed can take place individually or together, material is eroded by shear, fracture and plastic deformation of workpiece that will take place on top layer of the material. Material removal due to cavitation erosion is prone to occur on porous materials such as graphite compared with hardened steels. The fragments are later removed by liquid carrier [6, 104].

Abrasive particle raises tensile stress of workpiece when it impinges on top layer. Hence, micro cracks are located around

Fig. 45 Influence of tool diameter on MRR [106]

Fig. 46 Morphology of hole exit under high static load [102]

7.2 Tool wear

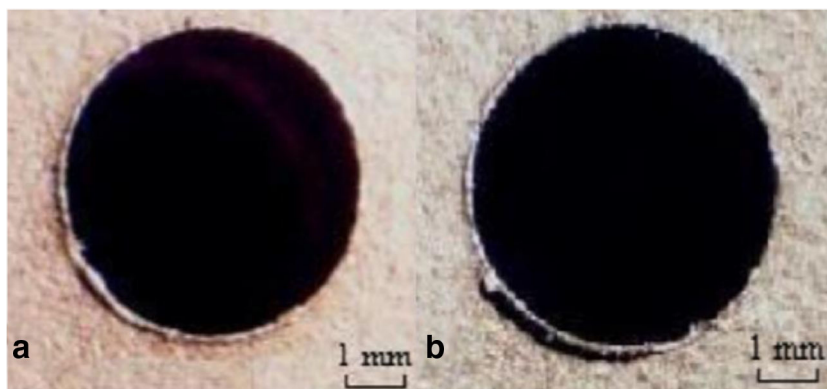Tool wear is an important issue for ultrasonic drilling as the performance and efficiency of drilling depends on it [105]. Tool wear is caused due to abrasive. As abrasive particle strikes on tool, cracking of tool material will start to occur followed by erosion and results in tool wear [106]. Cronjlger [107] in lateral and longitudinal directions. Where longitudinal wear decreases the length of tool due to consistent impact forces by abrasive particles, lateral or side wear decreases the diameter of tool from its initial condition because of the scraping of abrasive particles that occurs in the tiny space in the middle of tool and workpiece. Cavitation wear [108] might also occur due to quick return motion of tool that develops aggressive cavitation around bottom and side of tool. Bubbles consist of absorbed gases which creates strong currents that travel diagonally towards bottom of the tool and around the workpiece and causes cavitation wear. Factors like workpiece material and thickness, tool material and dimensions, size and type of abrasive particle, speed and technique of feeding slurry and cutting duration influence tool wear. Tools made of martensite steel were found to be superior than other materials in terms of wear resistance. Tool wear was found to be inversely proportion to tool hardness for tempered metals [109]. Adithan et al. [109] found that with same tool size, tool wear rate was higher when using boron carbide as compared with silicon carbide particles. Figure 42 shows how tool wear is affected by abrasive type. The reason is probably because of the hardness of grits, as metal removal rate depends on grit hardness. Furthermore, boron carbide damps quicker than silicon carbide, and dampness is a crucial factor for the development and breakdown of cavitation bubble which causes cavitation wear. Thus, tool wear will be higher when using boron carbide opposed to silicon carbide. Larger particles

the contact region gets aggravated. As soon as tensile stress elevates, tension acting on material increases, and crack located on contact region will begin to spread around drilling zone and form under top layers of the material to a certain depth. The depressed area depends on the magnitude of load, whereby an increase in load will increase crack around drilling zone and spread progressively in deeper layers of material. As soon as stress value reaches materials' failure point, round crack impinged by abrasive particle forms into a cone-shaped crack. As static load increases, crack continues to progress deeper in workpiece and contact area will then be bounded with cone shaped cracks. With constant impinge force and unloading, crack will start to get tighter and gradually form a round groove [104]. Figure 40 illustrates the erosion process by

Fig. 47 Exit of holes machined at **a** 250 rpm and feed rate if 0.8 mm/s and **a** 350 rpm and 0.5 mm/s feed rate [119]
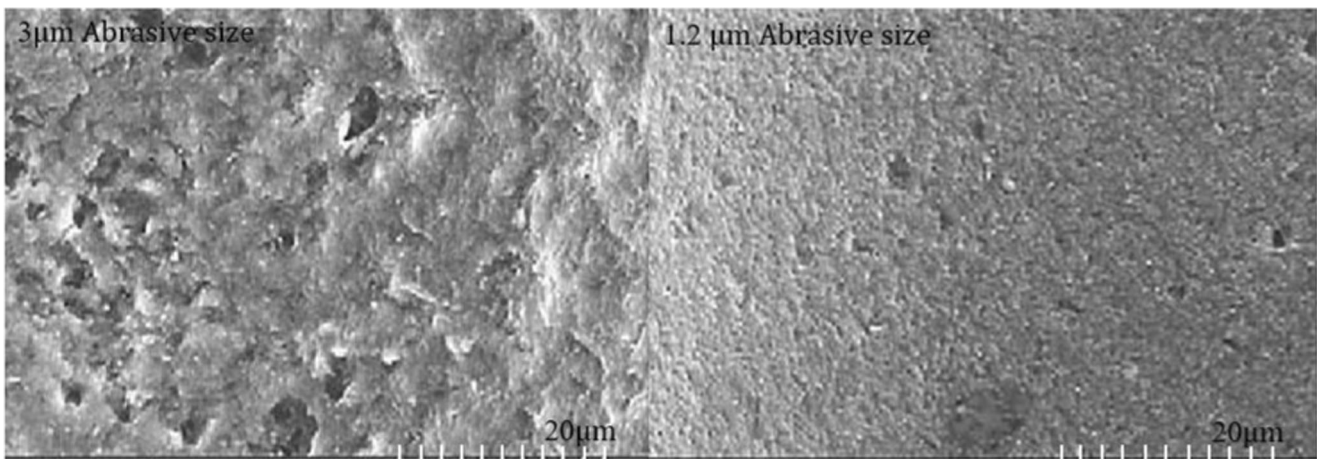
Fig. 48 Abrasive size influence on surface roughness of borosilicate glass workpiece [121]

create greater tool wear as opposed to finer particles as contact area of particle is larger for large particles and hence, fragmentation increases as compared to a smaller particle. Figure 42 presents the effect of tool material on tool wear where mild steel tool experienced highest wear as compared with the rest of the materials. On the other hand, stainless steel experienced least wear as stainless steel has greatest cavitation corrosion resistance compared to rest of the materials. A similar study was conducted by Dvivedi and Kumar [99] where the influence of tool materials such as high-speed steel, tungsten carbide and high carbon steel on wear resistance was investigated. Tools with high carbon content were reported to have higher resistance to wear. Komaraiah and Reddy [110] reported that mild steel tool experienced highest wear among titanium, stainless steel and silver steel tools.

Adithan [109] experimented on different materials such as plate glass and porcelain, with different abrasive type and size and different static loads to observe the influence on tool wear. The results indicated that tool wear increases with higher static loads for tools with smaller bottom surface area. As static load increases, pressure applied by tool increases, furthermore with smaller area, pressure is larger, hence tool wear rate increases. Similar results were obtained by Yu [106] where tool wear was reported to increase as the force applied on tool increases. Tool wear rate is dependent by the tool itself, as if wear has already taken place, then additional wear will take place which is also influenced by the initial surface condition of the tool [106].

A trend between different materials and tool wear rate was also investigated by Adithan [109] and found that when drilling porcelain and glass, tool wear rate was higher for porcelain than glass. As hardness of workpiece increases, tool wear rate was greater. This is probably because of the ease of deformation of workpiece and the force needed to deform workpiece. Porcelain has a higher resistance of deformation than glass, hence force needed from tool is higher which increases tool wear rate as shown in Fig. 43.

7.3 Material removal rate

Several factors affecting material removal rate of ultrasonic drilling have been analysed. Several studies found that main parameters affecting MMR include workpiece material and thickness, size and concentration of abrasive slurry, applied pressure, static load applied by tool and power of the machine.

Pandey and Shan [111] found that pressure of slurry flowing in cutting zone has an incredible influence on removal rate of both workpieces as with high pressure comes higher forces, abrasive particles will strike workpiece, hence increasing material removal rate. Hocheng et al. [102] investigated how different types of abrasive influences MRR. Experiment was conducted on carbon fibre-reinforced silicon carbide as workpiece material. Three different type of abrasive of same size (#220) were used namely B_4C, SiC and Al_2O_3. They also reported that material removal rate was highest when B_4C grits were used as it has highest hardness compared with other
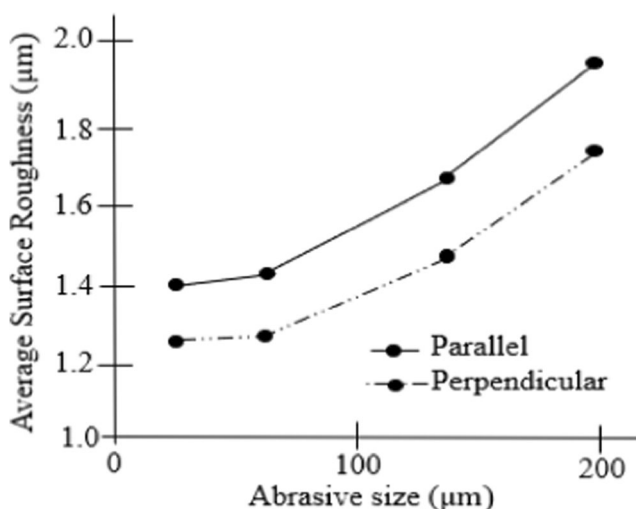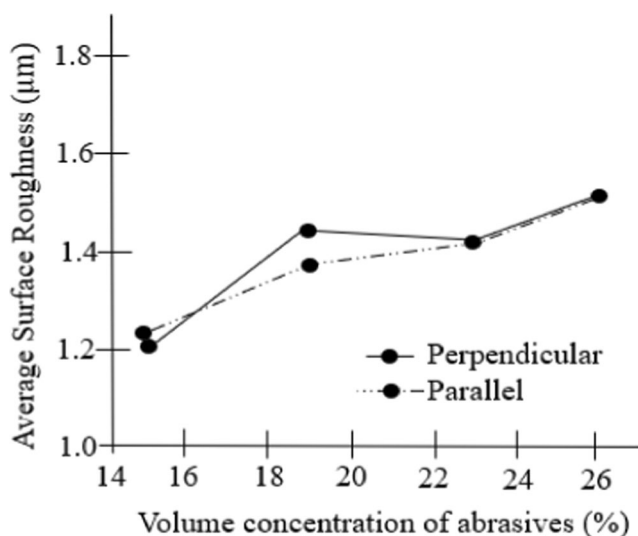

Fig. 49 Abrasive size influence on average surface roughness [120]

Fig. 50 Effect of abrasive slurry volume concentration on average surface roughness [120]

two abrasives. Abrasive size also affects material removal rate as coarser grits causes higher damage due to hammering effect of abrasives and hence increasing MRR [102]. Similar results were reported by Singh et al. [112] that the larger the size of grits, the higher is material removal rate as shown in Fig. 44 where abrasive particle size is approximately directly proportional to drilling speed.

Anantha et al. [114] investigated the influence of two different ceramic materials namely compact Alumina (Al_2O_3) and Zirconia (ZrO_2) on productivity of USD. It was reported that ZrO_2 with a higher hardness than Al_2O_3 resulted in lower material removal rate because of greater "bounce back" effect of abrasives that resulted in lesser erosion of workpiece [114]. Yu et al. [106] investigated the influence of tungsten tool size on material removal rate of silicon wafer where diameters of

the tool were 50, 100 and 150 mm. It was found that MRR increased when the diameter of tool increase, as large surface area of tool increases the size of working area and hence, more abrasive grain can join to remove the material. An example of the trend is shown in Fig. 45. Anantha et al. [114] reported that penetration rate is different for different type of materials. For this study, tool materials that were investigated were mild steel, stainless steel and high-speed steel, where stainless steel showed higher penetration rate compared to other two materials.

Number of studies [6, 115] reported linear relationships between material removal rate and tool frequency. This is possibly due to increase in amplitude. As vibration amplitude increases, rate at which material is removed also increases. This is because, with higher vibration, excitation energy of abrasive particles will be large, hence the impinging force on top layer of workpiece increases, resulting in higher rate of chipping of workpiece [6, 116]. Static load influences MRR as reported by Yu et al. [106], where static load increases material removal rate as the pressure that is applied on grits increases. Similar results were found by Hocheng et al. [102] where the increase in static load increases material removal rate as excitement force on abrasive increases with the rise of static load. Hence the impact force on workpiece exerted by abrasives increases. Studies conducted by various researchers [99, 117] also agree to a linear relationship with power rating of machine and material removal rate, where increase in power increases material removal rate as when power is surged, energy and momentum of abrasives are higher [117].

7.4 Hole characteristics and surface roughness

Accuracy and surface roughness of holes are based on major factors such as static load, slurry concentration, abrasive size

Table 1 Aspects of different drilling techniques [1, 2, 6, 9]

Drilling techniques characteristics	Electro discharge drilling	Electrochemical drilling	Ultrasonic drilling	Abrasive waterjet drilling	Laser drilling
Hole surface damage	Presence of heat affected zones and recast layer	Absence of heat-affected zones and recast layer	Absence of heat-affected zones and recast layer	Absence of heat-affected zones and recast layer	Heat-affected zones and recast layer present
Costs	High tool costs	Low set-up costs	Expensive equipment costs	High maintenance costs, high tool costs and high labour costs	Expensive machine and maintenance costs
Material removal rate	Slowest	Fast	Slow	Fast	Fast
Type of materials can be drilled	Only electrically conductive	Only electrically conductive	Materials with hardness above 40 HRC, including electrically conductive materials	Soft and hard materials, including electrically conductive materials	Non-reflective surface workpiece, including electrically conductive materials
Tool wear	Present	Absent	Present	Absent	Absent

and feed rate. Accuracy of hole can be assessed by their out-of-roundness and conical shape by measures taken at top and bottom diameters of hole. Adithan et al. [118] reported that size of abrasive particles had the most influence on drilling accuracy where finer particles result in higher accuracy holes with good improvement in circularity. This is because, when a large static load is applied, abrasive particles breakdown and reduces in size due to large force. As a result of the wear on abrasive particles, oversize of holes will decrease due to smaller abrasive particles. Hocheng et al. [102] found that delamination at the bottom hole increases with higher load. It is because during drilling process, size of exit hole is not big enough to push the material out from exit, hence deformations occur at exit hole. Best quality holes were found when using boron carbide as compared to silicon carbide and aluminium oxide as hardness of boron carbide is the highest compared to other two. An example of exit hole produced on carbon fibre reinforced with silicon carbide abrasive at high static load is shown in Fig. 46. Azarhoushang et al. [119] conducted ultrasonic drilling on Inconel 738-LC and found that influence of tool speed and feed rate has a small impact on hole quality as shown in Fig. 47.

Hocheng et al. [120] found that the main parameters affecting surface roughness of the holes are abrasive size, supplied current responsible for tool oscillations and slurry concentration. Surface roughness is proportional to abrasive as indent force will be greater. Hence, bigger area of crater will be formed on substrate. Thus, smoother surface was obtained with finer abrasive as compared to coarser ones. Examples of micro-hole surface with abrasive size of 3 and 1.2 μm is presented in Fig. 48. A similar trend was observed by Thoe et al. [6], where abrasive particle size and surface roughness are directly proportional as presented in Fig. 49. Figure 50 shows that with higher concentration of slurry, surface roughness increases due to higher dynamic energy of abrasives and hence larger shear force acting on substrate to generate higher roughness. The direction of fibres in workpiece in relation of drilling direction has an effect on surface as shown in Fig. 49. The reason for slight variation is because the direction in which abrasive is flowing influences fibres break out.

8 Conclusions

Many industries require to drill micro-holes with high dimensional accuracy together with high efficiency and speed. Mechanical stresses or burr formation on workpiece is undesired by many applications. The non-conventional drilling processes discussed in this paper are able to meet the demands of specific manufacturing industries. However, each process has its own advantages and disadvantages. In order to drill a hole with high accuracy, certain parameters of each process have to be optimized. The characteristics of different non-traditional drilling processes are summarized in Table 1.

Absence of materials' microstructure change, heat-affected zones and tool wear makes abrasive waterjet drilling preferable compared to other non-conventional methods such as EDM and laser beam drilling. Pressure of water, mass flow rates of abrasives, stand-off distance, material type and workpiece thickness affect drill time. The quality of holes and surface finish are affected by the pressure of jet, stand-off distance and type of material. The highest contribution to heat damage and micro cracking in laser drilling was due to the energy density of the beam. However, at higher energy, the material removal rate and the circularity of the hole was better. The current and the electrolyte concentration and flow rate were the most influential parameters in electrochemical drilling in terms of material removal and hole quality. Electric discharge has the largest contribution on hole quality during EDM drilling where the hole quality reduces with the increase of current. Desired hole characteristics can be achieved by controlling current, frequency, dielectric and electrode. In ultrasonic drilling, the load and abrasives are main contributor to the surface quality and the type of damage on the hole, when controlled, desired hole quality can be achieved.

9 Future work

The literature review presented in this paper has covered most of the non-conventional drilling methods. However, not all non-conventional drilling methods have been covered, such as electron beam drilling and some hybrid methods, due to the lack of studies and limited available research papers in this area. Thus, from future work aspects, looking into electron beam drilling and hybrid methods will be a potential area of interest, with the advancement of new systems.

References

1. Skoczypiec S et al (2015) The capabilities of electrodischarge microdrilling of high aspect ratio holes in ceramic materials. Manag Prod Eng Rev 6(3):61–69
2. Hasan M, Zhao J, Jiang Z (2017) A review of modern advancements in micro drilling techniques. J Manuf Process 29:343–375
3. Zhao W, Li X, and Wang Z. (2006) Study on micro electrochemical machining at micro to meso-scale. In 2006 1st IEEE international conference on Nano/micro engineered and molecular systems. IEEE
4. Suchánek L, Zetková I (2015) Evaluation of the surface small holes drilled by unconventional methods. Proc Eng 100:1582–1590
5. Zhang F, Zhu J (2013) An experimental study of drilling small and deep blind holes with an abrasive water jet. Springer Berlin Heidelberg, Berlin

6. Thoe TB, Aspinwall DK, Wise MLH (1998) Review on ultrasonic machining. Int J Mach Tools Manuf 38(4):239–255

7. Yilbas BS (2012) Laser drilling: practical applications. Springer Science & Business Media

8. Bellotti M, Qian J, Reynaerts D (2018) Enhancement of the micro-EDM process for drilling through-holes. Procedia CIRP 68(1):610–615

9. Sen M, Shan HS (2005) A review of electrochemical macro- to micro-hole drilling processes. Int J Mach Tools Manuf 45(2):137–152

10. Korat M, Acharya G (2014) A review on current research and development in abrasive waterjet machining. Int J Eng Res Appl 4(1):423–432

11. Hashish M, Whalen J (1993) Precision drilling of ceramic-coated components with abrasive-waterjets. J. Eng Gas Turbines Power 115(1):148–154

12. Parikh PJ, Lam SS (2009) Parameter estimation for abrasive water jet machining process using neural networks. Int J Adv Manuf Technol 40(5–6):497–502

13. Liu H-T (2007) Hole drilling with abrasive fluidjets. Int J Adv Manuf Technol 32(9):942–957

14. Kirk DJDU (2010) CSC publishing, powder and B. Engineering, A quick and easy formula for mesh-micron particle size conversions

15. Zohoor M, Nourian SH (2012) Development of an algorithm for optimum control process to compensate the nozzle wear effect in cutting the hard and tough material using abrasive water jet cutting process. Int J Adv Manuf Technol 61(9):1019–1028

16. Akkurt A (2009) The effect of material type and plate thickness on drilling time of abrasive water jet drilling process. Mater Des 30(3):810–815

17. Kulekci MK (2002) Processes and apparatus developments in industrial waterjet applications. Int J Mach Tools Manuf 42(12):1297–1306

18. Alberdi A et al (2016) An experimental study on abrasive waterjet cutting of CFRP/Ti6Al4V stacks for drilling operations. Int J Adv Manuf Technol 86(1):691–704

19. Ramulu M, Posinasetti P, and Hashish M (2005) Analysis of the abrasive waterjet drilling process. in 2005 WJTA American Waterjet Conference

20. Palleda M (2007) A study of taper angles and material removal rates of drilled holes in the abrasive water jet machining process. J Mater Process Technol 189(1):292–295

21. Guha A, Barron R, Balachandar R (2011) An experimental and numerical study of water jet cleaning process. J Mater Process Technol 211(4):610–618

22. Hunt D, Burnham C, and Kim T (1987) Surface finish characterization in machining advanced ceramics by abrasive waterjet. in Proceedings of the Fourth U. S. Water Jet Conference.

23. Hamatani G, Ramulu M (1990) and technology, Machinability of high temperature composites by abrasive waterjet. J Eng Mater Technol 112(4):381–386

24. Momber AW and Kovacevic R (2012) Principles of abrasive water jet machining. Springer London

25. Zhang, S., et al. (2005) Accurate hole drilling using an abrasive water jet in titanium. in American Waterjet conference

26. Liu H-T, Schubert E (2009) Piercing in delicate materials with abrasive-waterjets. Int J Adv Manuf Technol 42(3–4):263–279

27. Phapale K et al (2016) Delamination characterization and comparative assessment of delamination control techniques in abrasive water jet drilling of CFRP. Proc Manuf 5:521–535

28. Hashish M (1988) Machining of advanced composites with abrasive-waterjets. Machining composites p. 1–18

29. Davim JP, Reis P (2005) Damage and dimensional precision on milling carbon fiber-reinforced plastics using design experiments. J Mater Process Technol 160(2):160–167

30. Tam S et al (1993) Optimization of laser deep-hole drilling of Inconel 718 using the Taguchi method. J Mater Process Technol 37(1–4):741–757

31. Ghoreishi M et al (2002) Comparative statistical analysis of hole taper and circularity in laser percussion drilling. Int J Mach Tools Manuf 42(9):985–995

32. Kuar A et al (2006) Modelling and analysis of pulsed Nd: YAG laser machining characteristics during micro-drilling of zirconia (ZrO2). Int J Mach Tools Manuf 46(12–13):1301–1310

33. Forget P et al (1988) Laser drilling of a superalloy coated with ceramic. Mater Manuf Process 4(2):553–562

34. Gautam GD, Pandey AK (2018) Pulsed Nd: YAG laser beam drilling: a review. Opt Laser Technol 100:183–215

35. Wagner RE (1974) Laser drilling mechanics. J Appl Phys 45(10):4631–4637

36. Dubey AK, Yadava V (2008) Laser beam machining—a review. Int J Mach Tools Manuf 48(6):609–628

37. Majumder A (2010) Comparison of ANN with RSM in predicting surface roughness with respect to process parameters in Nd: YAG laser drilling. Int J Eng Sci Technol 2(10):5175–5186

38. Dhar S, Saini N, and Purohit R (2006) A review on laser drilling and its techniques. in International conference on advances in mechanical engineering

39. Pham DT, Dimov SS, Petkov PV (2007) Laser milling of ceramic components. Int J Mach Tools Manuf 47(3):618–626

40. Ready J (1964) Interaction of high power laser radiation with absorbing surfaces (high power laser radiation interaction with absorbing opaque surfaces, estimating temperature rise and depth of vaporized hole). in 20th National electronices conference, Chicago

41. Dabby F, Paek U-C (1972) High-intensity laser-induced vaporization and explosion of solid material. IEEE J Quantum Electron 8(2):106–111

42. Yilbas B (1997) Parametric study to improve laser hole drilling process. J Mater Process Technol 70(1–3):264–273

43. Yilbas B (1988) Investigation into drilling speed during laser drilling of metals. Opt Laser Technol 20(1):29–32

44. Yilbas BS (1987) Study of affecting parameters in laser hole drilling of sheet metals. J Eng Mater Technol 109(4):282–287

45. Mishra S, Yadava V (2013) Modeling and optimization of laser beam percussion drilling of thin aluminum sheet. Opt Laser Technol 48:461–474

46. Roos SO (1980) Laser drilling with different pulse shapes. J Appl Phys 51(9):5061–5063

47. Bandyopadhyay S et al (2002) Geometrical features and metallurgical characteristics of Nd:YAG laser drilled holes in thick IN718 and Ti–6Al–4V sheets. J Mater Process Technol 127(1):83–95

48. Wang H et al (2017) Laser drilling of structural ceramics—a review. J Eur Ceram Soc 37(4):1157–1173

49. Mishra S, Yadava VJMS (2013) And technology, modelling of hole taper and heat affected zone due to laser beam percussion drilling. Mach Sci Technol 17(2):270–291

50. Iwatani N, Doan HD, Fushinobu K (2014) Optimization of near-infrared laser drilling of silicon carbide under water. Int J Heat Mass Transf 71:515–520

51. Vora HD et al (2013) One-dimensional multipulse laser machining of structural alumina: evolution of surface topography. Int J Adv Manuf Technol 68(1):69–83

52. Kamlage G et al (2003) Deep drilling of metals by femtosecond laser pulses. Applied physics A 77(2):307–310

53. Luft A et al (1996) A study of thermal and mechanical effects on materials induced by pulsed laser drilling. Applied physics A 63(2):93–101

54. Low DKY, Li L, Byrd PJ (2000) The effects of process parameters on spatter deposition in laser percussion drilling. Opt Laser Technol 32(5):347–354

55. Rahman Z, Das AK, Chattopadhyaya S (2018) Microhole drilling through electrochemical processes: a review. Mater Manuf Process 33(13):1379–1405

56. Manikandan N, Kumanan S, Sathiyanarayanan C (2015) Multi response optimization of electrochemical drilling of titanium Ti6Al4V alloy using Taguchi based grey relational analysis. Indian J Eng Mater Sci 22(2):153–160

57. Bannard J (1979) Fine hole drilling using electrochemical machining, in proceedings of the nineteenth international machine tool design and research conference: held in Manchester, 13th – 15th September, 1978, B.J. Davies, Editor, Macmillan Education UK: London. p. 503–510

58. Sharma RD, Singh R, Singh M (2012) Study of electro-chemical machining process for drilling hole. Int J Eng Res Technol 1:1–5

59. Chryssolouris G, Wollowitz M, Sun N (1984) Electrochemical hole making. CIRP Ann 33(1):99–104

60. Ahn SH et al (2004) Electro-chemical micro drilling using ultra short pulses. Precis Eng 28(2):129–134

61. McGeough JA et al (2003) Recent research and developments in electrochemical machining. Int J Electricial Mach 8:1–14

62. Amalnik MS, McGeough JA (1996) Intelligent concurrent manufacturability evaluation of design for electrochemical machining. J Mater Process Technol 61(1):130–139

63. Wang X et al (2016) Electrochemical drilling with constant electrolyte flow. J Mater Process Technol 238:1–7

64. Noot MJ et al (1998) Real time numerical simulation and visualization of electrochemical drilling. Comput Vis Sci 1(2):105–111

65. Hocheng H et al (2003) A material removal analysis of electrochemical machining using flat-end cathode. J Mater Process Technol 140(1):264–268

66. Hewidy MS (2005) Controlling of metal removal thickness in ECM process. J Mater Process Technol 160(3):348–353

67. Mukherjee SK et al (2008) Effect of valency on material removal rate in electrochemical machining of aluminium. J Mater Process Technol 202(1):398–401

68. Mithu M, Fantoni G, Ciampi J (2011) The effect of high frequency and duty cycle in electrochemical microdrilling. Int J Adv Manuf Technol 55(9–12):921–933

69. Manna A and Malik A. (2016) Micro-drilling of Al/Al2O3-MMC on developed ECMM. in Proceedings of the world congress on engineering

70. Rao SR, Padmanabhan G (2012) Application of Taguchi methods and ANOVA in optimization of process parameters for metal removal rate in electrochemical machining of Al/5% SiC composites. Int J Eng Res Appl 2(3):192–197

71. Mithu M, Fantoni G, Ciampi J (2011) A step towards the in-process monitoring for electrochemical microdrilling. Int J Adv Manuf Technol 57(9–12):969

72. Goswami R et al (2013) Optimization of electrochemical machining process parameters using Taguchi approach. Int J Eng Sci Technol 5(5):999

73. Thanigaivelan R, Arunachalam R, Drukpa P (2012) Drilling of micro-holes on copper using electrochemical micromachining. Int J Adv Manuf Technol 61(9–12):1185–1190

74. da Silva Neto JC, Da Silva EM, Da Silva MB (2006) Intervening variables in electrochemical machining. J Mater Process Technol 179(1–3):92–96

75. Zhu D, Xu HY (2002) Improvement of electrochemical machining accuracy by using dual pole tool. J Mater Process Technol 129(1):15–18

76. Qu NS et al (2013) Enhancement of surface roughness in electrochemical machining of Ti6Al4V by pulsating electrolyte. Int J Adv Manuf Technol 69(9):2703–2709

77. Pham DT et al (2007) An investigation of tube and rod electrode wear in micro EDM drilling. Int J Adv Manuf Technol 33(1):103–109

78. Yilmaz O, Okka MA (2010) Effect of single and multi-channel electrodes application on EDM fast hole drilling performance. Int J Adv Manuf Technol 51(1):185–194

79. Lim HS et al (2003) A study on the machining of high-aspect ratio micro-structures using micro-EDM. J Mater Process Technol 140(1):318–325

80. Ay M, Çaydaş U, Hasçalık A (2013) Optimization of micro-EDM drilling of inconel 718 superalloy. Int J Adv Manuf Technol 66(5):1015–1023

81. Diver C et al (2004) Micro-EDM drilling of tapered holes for industrial applications. J Mater Process Technol 149(1):296–303

82. Ho KH, Newman ST (2003) State of the art electrical discharge machining (EDM). Int J Mach Tools Manuf 43(13):1287–1300

83. Kunieda M et al (2005) Advancing EDM through fundamental insight into the process. CIRP Ann 54(2):64–87

84. Rajurkar KP, Sundaram MM, Malshe AP (2013) Review of electrochemical and electrodischarge machining. Procedia CIRP 6:13–26

85. D'Urso G, Maccarini G, Ravasio C (2014) Process performance of micro-EDM drilling of stainless steel. Int J Adv Manuf Technol 72(9):1287–1298

86. Kibria G et al (2010) Comparative study of different dielectrics for micro-EDM performance during microhole machining of Ti-6Al-4V alloy. Int J Adv Manuf Technol 48(5):557–570

87. Jilani ST, Pandey PC (1984) Experimetnal investigations into the performance of water as dielectric in EDM. Int J Mach Tool Des Res 24(1):31–43

88. Klink A (2014) Electric discharge machining. In: Laperrière L, Reinhart G (eds) CIRP Encyclopedia of production engineering. Springer Berlin Heidelberg, Berlin, pp 439–443

89. Mohri N et al (1995) Electrode wear process in electrical discharge machinings. CIRP Ann 44(1):165–168

90. Jahan MP, Wong YS, Rahman M (2010) A comparative experimental investigation of deep-hole micro-EDM drilling capability for cemented carbide (WC-Co) against austenitic stainless steel (SUS 304). Int J Adv Manuf Technol 46(9):1145–1160

91. Janmanee P and Muttamara A, (2011) A study of hole drilling on stainless steel AISI 431 by EDM using brass tube electrode. Int Trans J Eng Manag Appl Sci Technol

92. Kuppan P, Rajadurai A, Narayanan S (2008) Influence of EDM process parameters in deep hole drilling of Inconel 718. Int J Adv Manuf Technol 38(1–2):74–84

93. Liu H-S et al (2005) A study on the characterization of high nickel alloy micro-holes using micro-EDM and their applications. J Mater Process Technol 169(3):418–426

94. Mathew J et al (2008) Effect of work material and machining conditions on the efficiency and accuracy of micro electric discharge drilling, Proceedings of 8th APCMP, China, pp 550–558

95. Mohan B, Rajadurai A, Satyanarayana K (2002) Effect of SiC and rotation of electrode on electric discharge machining of Al–SiC composite. J Mater Process Technol 124(3):297–304

96. Neppiras E, Foskett R (1957) Ultrasonic machining-II. Operating conditions and performance of ultrasonic drills. Philips technology review 18(12):368–379

97. Gilmore R, Ultrasonic machining of ceramics. 1990: Society of manufacturing engineers

98. Kennedy D, Grieve R (1975) Ultrasonic machining-a review. Prod Des Eng 54(9):481–486

99. Dvivedi A, Kumar P (2007) Surface quality evaluation in ultrasonic drilling through the Taguchi technique. Int J Adv Manuf Technol 34(1):131–140

100. Moreland M (1991) Ultrasonic machining—book chapter: ceramics and glasses. ASM Int Eng Mater Handbook ISBN 871702827:359–362

101. Drozda T and Wick C, (1983) Non-traditional machining. Soc Manuf Eng. p. 1–23

102. Hocheng H, Tai NH, Liu CS (2000) Assessment of ultrasonic drilling of C/SiC composite material. Compos A: Appl Sci Manuf 31(2):133–142

103. Wiercigroch M, Neilson RD, Player MA (1999) Material removal rate prediction for ultrasonic drilling of hard materials using an impact oscillator approach. Phys Lett A 259(2):91–96

104. Ya G et al (2002) Analysis of the rotary ultrasonic machining mechanism. J Mater Process Technol 129(1):182–185

105. Adithan M, Venkatesh VC (1974) Parameter influence on tool wear in ultrasonic drilling. Tribology 7(6):260–264

106. Yu Z, Rajurkar K, Tandon A (2004) Study of 3D micro-ultrasonic machining. J Manuf Sci Eng 126(4):727–732

107. Cronjlger L (1961) Einsenken unter Ultraschalleinwirkung. Diss TH, Hannover

108. Riddei V, Roch G (1973) Cavitation erosion—a survey of the literature 1940–1970. Wear 23(1):133–136

109. Adithan M (1974) Tool wear studies in ultrasonic drilling. Wear 29(1):81–93

110. Komaraiah M, Reddy PN (1993) Relative performance of tool materials in ultrasonic machining. Wear 161(1):1–10

111. Pandey PC and Shan H (1980) Modern machining processes. Tata McGraw-Hill Education

112. Singh R, Khamba JS (2006) Ultrasonic machining of titanium and its alloys: a review. J Mater Process Technol 173(2):125–135

113. Miller GE (1957) Special theory of ultrasonic machining. J Appl Phys 28(2):149–156

114. Anantha Ramu BL, Krishnamurthy R, Gokularathnam CV (1989) Machining performance of toughened zirconia ceramic and cold compact alumina ceramic in ultrasonic drilling. J Mech Work Technol 20:365–375

115. Goetze D (1956) Effect of vibration amplitude, frequency, and composition of the abrasive slurry on the rate of ultrasonic machining in ketos tool steel. J Acoust Soc Am 28(6):1033–1037

116. McGeough JA (1988) Advanced methods of machining. Springer Science & Business Media

117. Singh R, Khamba JS (2008) Comparison of slurry effect on machining characteristics of titanium in ultrasonic drilling. J Mater Process Technol 197(1):200–205

118. Adithan M, Venkatesh VC (1976) Production accuracy of holes in ultrasonic drilling. Wear 40(3):309–318

119. Azarhoushang B, Akbari J (2007) Ultrasonic-assisted drilling of Inconel 738-LC. Int J Mach Tools Manuf 47(7):1027–1033

120. Hocheng H, Hsu CC (1995) Preliminary study of ultrasonic drilling of fiber-reinforced plastics. J Mater Process Technol 48(1): 255–266

121. Yan BH et al (2002) Study of precision micro-holes in borosilicate glass using micro EDM combined with micro ultrasonic vibration machining. Int J Mach Tools Manuf 42(10):1105–1112